Physica D ▮ (▮▮▮▮) ▮▮▮–▮▮▮

Contents lists available at SciVerse ScienceDirect

Physica D

journal homepage: www.elsevier.com/locate/physd

Stochastic climate dynamics: Random attractors and time-dependent invariant measures

Mickaël D. Chekroun [a,b,*], Eric Simonnet [c], Michael Ghil [a,b,d]

[a] Department of Atmospheric Sciences and Institute of Geophysics and Planetary Physics, University of California, Los Angeles, CA 90095-1565, USA

[b] Environmental Research and Teaching Institute (CERES-ERTI), École Normale Supérieure, 75231 Paris Cedex 05, France

[c] Institut Non Linéaire de Nice (INLN)-UNSA, UMR 6618 CNRS, 1361, route des Lucioles 06560 Valbonne, France

[d] Geosciences Department and Laboratoire de Météorologie Dynamique (CNRS and IPSL), École Normale Supérieure, 75231 Paris Cedex 05, France

ARTICLE INFO

Article history:
Received 8 January 2010
Received in revised form
1 June 2011
Accepted 3 June 2011
Available online xxxx
Communicated by H.A. Dijkstra

Keywords:
Climate dynamics
Dissipative dynamical systems
Intermittency
Pullback and random attractor
Sample invariant measure
SRB measure

ABSTRACT

This article attempts a unification of the two approaches that have dominated theoretical climate dynamics since its inception in the 1960s: the nonlinear deterministic and the linear stochastic one. This unification, via the theory of random dynamical systems (RDS), allows one to consider the detailed geometric structure of the random attractors associated with nonlinear, stochastically perturbed systems. We report on high-resolution numerical studies of two idealized models of fundamental interest for climate dynamics. The first of the two is a stochastically forced version of the classical Lorenz model. The second one is a low-dimensional, nonlinear stochastic model of the El Niño–Southern Oscillation (ENSO). These studies provide a good approximation of the two models' global random attractors, as well as of the time-dependent invariant measures supported by these attractors; the latter are shown to have an intuitive physical interpretation as random versions of Sinaï–Ruelle–Bowen (SRB) measures.

1. Introduction and motivation

The geometric [1] and the ergodic [2] theory of dynamical systems represent a significant achievement of the last century. In the meantime, the foundations of the stochastic calculus also led to the birth of a rigorous theory of time-dependent random phenomena. Historically, theoretical developments in climate dynamics have been largely motivated by these two complementary approaches, based on the work of Lorenz [3] and that of Hasselmann [4], respectively [5].

It now seems clear that these two approaches complement, rather than exclude each other. Incomplete knowledge of small-, subgrid-scale processes, as well as computational limitations will always require one to account for these processes in a stochastic way. As a result of sensitive dependence on initial data and on parameters, numerical weather forecasts [6] as well as climate projections [7] are both expressed these days in probabilistic terms. In addition to the intrinsic challenge of addressing the nonlinearity along with the stochasticity of climatic processes, it is thus more convenient – and becoming more and more necessary – to rely on a model's (or set of models') probability density function (PDF) rather than on its individual, pointwise simulations or predictions; see e.g. [8–12] and references therein.

We show in this paper that finer, highly relevant and still computable statistics exist for stochastic nonlinear systems, which provide meaningful physical information not described by the PDF alone. These statistics are supported by a random attractor that extends the concept of a strange attractor [3,13] and of its invariant measures [2] from deterministic to stochastic dynamics.

The attractor of a deterministic dynamical system provides crucial geometric information about its asymptotic regime as $t \to \infty$, while the Sinaï–Ruelle–Bowen (SRB) measure provides, when it exists, the statistics of the flow over this attractor [2,14]. These concepts have been applied to climate dynamics – across a full hierarchy of models, from conceptual "toy" models via so-called intermediate models and all the way to high-resolution general circulation models (GCMs) – as well as to the related uncertainties [15–17]. Recent applications of ergodic theory to the problem of climate sensitivity, in the context of deterministic models of small and intermediate complexity, include [18–22].

On the stochastic side, the crucial field of modeling subgrid-scale phenomena has been increasingly moving toward stochastic

* Corresponding author at: Department of Atmospheric Sciences and Institute of Geophysics and Planetary Physics, University of California, Los Angeles, CA 90095-1565, USA.
E-mail address: mchekroun@atmos.ucla.edu (M.D. Chekroun).

0167-2789/$ – see front matter © 2011 Elsevier B.V. All rights reserved.
doi:10.1016/j.physd.2011.06.005

"parameterizations" [23,24]. Such parameterizations have been studied in terms of their impact on the successful simulation of certain physical processes in GCMs, but not in terms of their global impact on model behavior. At a more fundamental level, the climate system is an open system and subject to variable forcing in time. The long-term effects of time-dependent forcing, whether deterministic or stochastic, have only started to be studied; examples include Quaternary glaciations and their relationship to orbital forcing [25,26] or the interaction between the seasonal forcing and intrinsic variability in the Tropical Pacific [27,28].

During the past two decades, the mathematical theory of random dynamical systems (RDS) [29] and of nonautonomous dynamical systems [30] has made substantial progress in describing the asymptotic behavior of open systems, subject to time-dependent forcing. The pertinent mathematical literature, however, is fairly technical and opaque. Its concepts and methods have, therefore, not become widely understood and applied to the physical sciences in general and to climate dynamics in particular; see [31] and references therein.

The main objective of this paper is twofold: (i) to introduce the key concepts and tools of RDS theory – from the point of view of ergodic theory [2,14] – to a wider audience in the geosciences and macroscopic physics; and (ii) to present novel results for two highly idealized models of fundamental interest for climate dynamics. The first is a stochastically forced version of the Lorenz [3] model: We provide detailed geometric structure and novel statistical information by using a highly accurate numerical approximation of its global random attractor and of the invariant measures supported thereon; furthermore, these measures – called here sample measures [14] for short – are shown to be random SRB measures [32]. The second one is a low-dimensional, nonlinear stochastic El Niño–Southern Oscillation (ENSO) model [33]. Here we show how the information conveyed by its random attractor and sample measures allow one to better understand the qualitative behavior of this model – in particular its low-frequency variability (LFV) – and to refine its physical interpretation.

The paper is organized as follows. In Section 2, we introduce the pullback approach for nonautonomous dissipative dynamical systems and their pullback attractors. This is followed in Section 3 by the corresponding definitions and concepts for random forcing, in the setting of the ergodic theory of dynamical systems and while stressing the role of the sample measures. Numerical results on the sample measures for our two stochastic nonlinear models are presented in Section 4. These results are based on a random version of the SRB property, and provide geometric and probabilistic insights into the dynamics. Concluding remarks follow in Section 5. The mixing properties and decay of correlations used in the discussion of the stochastic ENSO model are clarified in Appendix A. In Appendix B, we attempt to provide a mathematically rigorous description of LFV, based on mixing ideas. Appendix C provides a rigorous justification of using the sample measures as random SRB measures.

In order to keep the presentation accessible to the intended audience, we refer for technical details to Arnold's [29] and Crauel's [34] books. For the sake of brevity, statements about the rigorous existence of the mathematical objects being described are typically omitted, while the three appendices provide brief definitions and explanations of key concepts, on both the mathematical and the climate side.

2. Forward approach *versus* pullback approach

What is the effect of random perturbations on a nonlinear deterministic system's phase portrait? To address this issue, especially in the case of a deterministically chaotic and dissipative system, we introduce herewith the appropriate framework. The discussion is developed in a finite dimensional context.

2.1. The classical forward approach

To analyze the effect of the noise on the invariant measure supported by the deterministic system's attractor, the traditional stochastic approach is to seek the fixed point of the associated Markov semigroup, i.e. to find stationary solutions of the Fokker–Planck equation. These solutions correspond precisely to the system's stationary measures. Numerically, it is most often easier to integrate the system forward in time, perform ensemble or time averages and call the resulting object the "PDF".

When a deterministic system is perturbed by noise, it is often observed that the support of such a numerically obtained PDF corresponds to a (small) phase-space neighborhood of the deterministic attractor; in particular, the topological structure of the deterministic attractor becomes fuzzy. Such an approach provides, therefore, purely statistical information, without a close link with the attractor's geometry. Even so, the effect of the noise can result in surprising changes, especially when the deterministic system is neither hyperbolic [35] nor stochastically stable [14].

The RDS approach is based on a drastically different view. Its fundamental objects are the random invariant measures of the dynamics rather than the stationary ones of the Markov semigroup. These invariant measures are supported by a well-defined attractor, as will be explained below. In this approach, instead of integrating forward in time, the system is run from a distant point s in the past until the present time t, where it is "frozen". We refer to this as the *pullback approach*. Remarkably, by looking at the system in this way, the topological structures related to the stochastic dynamics emerge naturally and, even more surprisingly, there is no fuzziness in them. RDS theory thus reconciles the ergodic and geometric approaches in the stochastic context. We explain next the pullback approach, what an RDS and a random attractor are, and discuss the invariant measures such an attractor supports.

2.2. The pullback approach

This approach adopts a pathwise analysis, rather than the previous one, based on an ensemble of realizations. At first glance, this angle of attack may appear more laborious and less direct in providing statistical information. In fact, it yields much more detailed insights, along with the PDF, as will be seen below.

To understand this relatively novel approach, we first explain heuristically the concept of pullback attractor in the context of a deterministic, but nonautonomous dynamical system. For simplicity, we consider a finite-dimensional system, written in the form,

$$\dot{\mathbf{x}} = \mathbf{f}(t, \mathbf{x}), \tag{1}$$

where the law $\mathbf{f}$ governing the evolution of the state $\mathbf{x}$ depends explicitly on time t.

A simple example from climate dynamics is given by the oceans' wind-driven circulation [36]. The effect of the atmosphere on the mid-latitude oceans at zero order would be modeled by a time-independent forcing that yields an autonomous system [31]. At the next order, however, taking into account the seasonal cycle in the winds, the forcing would become time periodic and the system thus nonautonomous [37]. As the degree of realism increases – unless one were to switch to a fully coupled atmospheric–ocean model – the time-dependent aspects would become more and more elaborate and involve not only the forcing but also various coefficients, which eventually will include stochastic effects at some point. Another example that will be illustrated in the numerical section of this paper is an ENSO model, in which wind bursts are modeled stochastically; see e.g. [38–40].

Stochastic models, in particular, are nonautonomous, rough rather than smooth, and are indexed by the realizations of the random processes involved.

Please cite this article in press as: M.D. Chekroun, et al., Stochastic climate dynamics: Random attractors and time-dependent invariant measures, Physica D (2011), doi:10.1016/j.physd.2011.06.005

For such models, we ask the following question:

Q: For a fixed realization ω, and at a fixed time t – the time at which the system is observed – how does the "stochastic flow" transform the Lebesgue measure on the phase space, assuming we have started the system in the asymptotic past?

It is this question that motivates and guides our exposition, and our subsequent results. This question will be handled for systems which contract the phase-space volume in an appropriate sense.

To study **Q**, we need to recall several concepts. First, let us denote by $\varphi(s,t)\mathbf{x}$ the solution of (1) at time t, where $\mathbf{x}$ is the initial state at time $s \leq t$, i.e. $\varphi(s,s)\mathbf{x} = \mathbf{x}$. In general, the operator $\varphi(s,t)$ generates a two-parameter semigroup that provides a two-time description of the system's evolution, while in the autonomous case a one-parameter semigroup suffices to entirely determine this evolution. In the latter case, the system's evolution is invariant with respect to translation in time, i.e. $\varphi(s,t)\mathbf{x} = \varphi(t-s)\mathbf{x}$, while in the former, the time at which initial data are prescribed is of paramount importance. Thus, in the nonautonomous case, the limiting behavior when $s \to -\infty$ and t is fixed may differ from the one obtained in the forward situation, with $t \to \infty$ and s fixed, whereas in the autonomous case the two limits represent the same asymptotic behavior, due to the translation invariance of $\varphi(s,t) = \varphi(t-s)$.

To illustrate the fundamental character of this distinction, consider the simple scalar version of (1): $\dot{x} = -\alpha x + \sigma t$, with $\alpha > 0$, and $\sigma \geq 0$. We denote again by $\varphi(s,t)x_0$ the solution at time t, assuming that $x(s) = x_0$ at $s \leq t$. The forward approach yields blow-up as $t \to +\infty$ for any x_0, while an easy computation shows that $|\varphi(s,t)x_0 - \mathcal{A}(t)| \to 0$ as $s \to -\infty$, for all t and x_0, with $\mathcal{A}(t) := \sigma(t - 1/\alpha)/\alpha$.

It can be shown further that $\mathcal{A}(t)$ is invariant under the dynamics, i.e. $\varphi(s,t)\mathcal{A}(s) = \mathcal{A}(t)$, for every $s \leq t$. We have therefore exhibited a family of limiting objects $\mathcal{A}(t)$, which exist in actual time t rather than asymptotically in the future, and which convey the effect of the dissipation due to the term $-\alpha x$. In this example, $\mathcal{A}(t)$ is simply a time-dependent point that attracts all the initial data.

More generally, in the forced dissipative case, one obtains for all t, by letting $s \to -\infty$, a collection $\bigcup_{t\in\mathbb{R}} \mathcal{A}(t)$ of objects $\mathcal{A}(t)$ that depend on time t; this collection is called a *pullback attractor*. Each $\mathcal{A}(t)$ may be more complicated than a point, and attract some subsets of initial data taken in the asymptotic past. In rigorous terms, a family of objects $\bigcup_{t\in\mathbb{R}} \mathcal{A}(t)$ in a finite-dimensional, complete metric phase space X is a pullback attractor if it satisfies the two following conditions:

(I) For all t, $\mathcal{A}(t)$ is a compact subset of X and is invariant with respect to the dynamics, namely,

$$\varphi(s,t)\mathcal{A}(s) = \mathcal{A}(t), \quad \text{for every } s \leq t; \quad \text{and}$$

(II) for all t, pullback attraction occurs:

$$\lim_{s\to-\infty} d_X(\varphi(s,t)B, \mathcal{A}(t)) = 0, \quad \text{for all } B \in \mathbb{B}. \tag{2}$$

In Eq. (2), $d_X(E,F)$ denotes the Hausdorff semi-distance

$$d_X(E,F) := \sup_{\mathbf{x}\in E} d_X(\mathbf{x},F), \quad \text{with } d_X(\mathbf{x},F) := \inf_{\mathbf{y}\in F} d(\mathbf{x},\mathbf{y}),$$

between the subset E and the subset F in X; here d is the metric in X, and the collection $\mathbb{B}$ of sets in X may itself exhibit some time dependence [29,30]. Note that, in general, $d_X(E,F) \neq d_X(F,E)$ and that $d_X(E,F) = 0$ implies $E \subset F$.

A fundamental property of a system's pullback attractor is that it may support physically interesting invariant measures. In the present paper, this aspect is discussed in greater detail for stochastically perturbed systems. We provide here a simple deterministic, but nonautonomous illustration.

Going back to $\dot{x} = -\alpha x + \sigma t$, one can show that every x-interval in $\mathbb{R}$, taken at a time $s < t$, shrinks onto $\mathcal{A}(t)$ as $s \to -\infty$. In terms of measure, one can say that the Dirac measure $\delta_{\mathcal{A}(t)}$, supported by $\mathcal{A}(t)$, "pullback attracts" at time t the Lebesgue measure on $\mathbb{R}$. By invariance of $\mathcal{A}(t)$, $\delta_{\mathcal{A}(t)}$ is thus a globally stable, time-dependent, invariant measure of our scalar nonautonomous system, just as δ_0 is for the autonomous system $\dot{x} = -\alpha x$, when $\sigma = 0$.

In general, the simplest and most fundamental measures that are invariant under the dynamics are precisely these time-dependent invariant Dirac measures. For a nonautonomous system, they replace the role played by fixed points for autonomous ones: time dependence usually prevents the system from being at rest and traditional fixed points become the exception, rather than the rule.

It follows that, if a nonautonomous dynamical system involves dissipation, we may wish to consider its asymptotic behavior in a pullback sense. Indeed, dissipative properties, coupled with time-dependent forcing, lead to the existence of a dynamical object $\bigcup_{t\in\mathbb{R}} \mathcal{A}(t)$, rather than a static one; this pullback attractor describes the asymptotic regime at time t, by considering the system initialized in the asymptotic past. Furthermore, this object supports invariant measures that are time-dependent by nature. At this stage, we have traveled half the road that leads to answering question **Q**. We need now to consider the random case, in order to travel the other half.

3. Noise effect on model statistics: a change of paradigm

3.1. The RDS approach

When the time-dependent forcing is random, the pullback attractor becomes a random pullback attractor or *random attractor* for short. This concept, however, is subtler than its "deterministic cousin" just discussed, and needs further clarification. In the 1980's, Kunita [41], among others, took an important step toward a geometrical description of "stochastic flows" by providing a pathwise two-parameter framework for describing the stochastic flows generated by fairly general stochastic differential equations (SDEs).

Roughly speaking, this framework allows one to show that, for almost all realizations ω living in some probability space Ω, the evolution in the phase space X of a stochastic system from time $s < t$ to time t is described by a two-parameter family of transformations $\varphi(s,t;\omega)$. It is tempting, therefore, to adopt the pullback approach just described above in an ω-parameterized version, in order to introduce the analog of a pullback attractor into the stochastic context. The problem with such a naive generalization is that the resulting object $\bigcup_{t\in\mathbb{R}} \mathcal{A}(t;\omega)$ does not exhibit any *a priori* relation between distinct realizations ω. As a matter of fact, this is one of the reasons why traditional approaches consider only expectations, i.e. ensemble means, rather than the stochastic flows.

The remedy to this problem comes from physical considerations. For an experiment to be repeatable, one has to have a reasonable description of its random aspects. These aspects may change in time, and thus the noise has to be modeled as a time-dependent stochastic process with certain known properties.

Representing mathematically such a stochastic process starts with a probability space $(\Omega, \mathcal{F}, \mathbb{P})$, where $\mathcal{F}$ is a σ-algebra of measurable subsets of Ω, called "events", and $\mathbb{P}$ is the probability measure [29]. Parameterizing noise by time, or equivalently, parameterizing the probability space by time, means that we should be able to connect the state ω of the random environment at time $t = 0$, say, with its state after a time t has elapsed; we call this connection $\theta_t\omega$ and set, of course, $\theta_0\omega = \omega$. This setup establishes a map $\theta_t : \Omega \mapsto \Omega$ for all times t.

Please cite this article in press as: M.D. Chekroun, et al., Stochastic climate dynamics: Random attractors and time-dependent invariant measures, Physica D (2011), doi:10.1016/j.physd.2011.06.005

In practice, one requires $(t, \omega) \mapsto \theta_t\omega$ to be measurable, and to satisfy the one-parameter group property $\theta_{s+t} = \theta_s \circ \theta_t$ for any s and t; along with $\theta_0 = \mathrm{id}_\Omega$, these requirements lead to a time-dependent family $\{\theta_t\}$ of invertible transformations of Ω that keeps track of the noise. Furthermore, one requires a stationarity condition, namely that the statistics of the external noise are invariant under θ_t; mathematically, this means that the probability measure $\mathbb{P}$ is preserved by θ_t, i.e. $\theta_t\mathbb{P} = \mathbb{P}$.

No other properties are needed in general: even ergodicity of θ_t appears to be secondary [29]. A simple example is given by the class of two-sided Wiener processes that are so pervasive in SDEs, where $\Omega = \{W \in C_0(\mathbb{R}), W(0) = 0\}$, while θ_t is the shift operator that acts according to $W_s(\theta_t\omega) = W_{s+t}(\omega) - W_t(\omega)$ making the Wiener process a helix over θ, and thus preserves the Wiener measure. In this particular case, ergodicity holds [29].

At this stage, we realize that the evolution of a stochastic system $\varphi(s, \tau; \omega)$ for $\tau > s$ can be derived from a simpler description $\Phi(t, \omega)$; this operator is parameterized by a single time variable t and it ascribes the state of the system at any time $t > 0$, starting at time $s = 0$ and given a realization ω that characterizes the state of the noise at time 0. Indeed, given the one-parameter mapping $\Phi(t, \omega)$, it is easy to obtain the evolution of the system from any time s to any time τ via the two-parameter mapping $\varphi(s, \tau; \omega) = \Phi(\tau - s, \theta_s\omega)$.

This simplification allows one to understand why a pathwise approach to modeling the noise may be reasonable: a system influenced by an external stochastic process for a single realization ω can be interpreted via the *driving system* $\{\theta_t\}$ as wandering along a path $\theta_t\omega$ in Ω and thus may provide additional statistical information to the modeler. For this to hold true, however, one must show that the system's behavior can be described in a self-consistent manner along such a path $\theta_t\omega$; this is the case if the stochastic dynamics $\Phi(t, \omega)$ satisfies the so-called *cocycle property*, namely $\Phi(t + s, \omega) = \Phi(t, \theta_s\omega) \circ \Phi(s, \omega)$ for all t, s and all ω, [29,31], in which case $\Phi(t, \omega)$ itself is called a perfect *cocycle*. Remarkably, RDS theory shows that the cocycle property holds for a very large class of random systems that includes standard SDEs; this result is mainly due to the group and measurability properties of $\{\theta_t\}$ associated with an attentive care of the exceptional sets [29]. In short, fairly general SDEs generate RDSs.

The cocycle concept lies at the core of RDS theory, thus extending Kunita's results [41]. It appears that the system $\Theta(t) : (\omega, x) \mapsto (\theta_t\omega, \Phi(t, \omega)x)$, also referred to as *a skew product*, is indeed a dynamical system on the extended phase space $\Omega \times X$, i.e. (probability space)×(phase space). We can thus deal with a genuine stochastic flow on this extended space, where $\Theta(t + s) = \Theta(t) \circ \Theta(s)$ holds. The notion of stochastic flow mentioned in question **Q** is therewith defined rigorously. One thus recovers much of the classical theory for autonomous flows, although there is an additional difficulty. This difficulty arises because, in the extended phase space $\Omega \times X$, one can only use measurability concepts on Ω, without any topological tools. The pair (Φ, θ) is called an RDS [29].

3.2. Random attractor

With these concepts and tools in hand, we are now in a position to extend the notion of pullback attractor to the stochastic context. To do so, consider first the classical Langevin equation,

$$dx = -\alpha x dt + \sigma dW_t, \quad \text{with } \alpha > 0 \text{ and } \sigma \neq 0. \tag{3}$$

Using stochastic calculus, the properties of the Wiener process and the definition of θ_t as a shift introduced above, it follows that $|\Phi(t, \theta_{-t}\omega)x - a(\omega)| \to 0$ as $t \to +\infty$; here $a(\omega) := \sigma \int_{-\infty}^{0} \exp(\alpha\tau) dW_\tau(\omega)$ and $\Phi(t, \omega)$ as defined above. The random variable a is even invariant under the dynamics, i.e. $\Phi(t, \omega)a(\omega) = a(\theta_t\omega)$, for all $t \geq 0$ and all $\omega \in \Omega$.

We have thus exhibited a family of random invariant objects – each of which is a single point $a(\omega)$ – that describe the possible states that can be observed in the present, at $t = 0$, whatever the state it occupied in the infinitely distant past, at $t = -\infty$. This contraction of the Lebesgue measure under the stochastic flow results, once more, from the effect of the dissipation that is "experienced" by the system in a pullback sense.

More generally, if a random subset $\mathcal{A}(\omega)$ of X satisfies certain measurability conditions [29], and furthermore

(I′) $\mathcal{A}(\omega)$ is a compact subset of X and Φ-invariant, i.e., for each $t \geq 0$, $\Phi(t, \omega)\mathcal{A}(\omega) = \mathcal{A}(\theta_t\omega)$; and
(II′) $\mathcal{A}(\omega)$ is attracting in the pullback sense, i.e.,

$$\lim_{t\to+\infty} d_X(\varphi(t, \theta_{-t}\omega)B(\theta_{-t}\omega), \mathcal{A}(\omega)) = 0, \quad \text{for all } B \in \mathbb{B},$$

then $\bigcup_{\omega\in\Omega} \mathcal{A}(\omega)$ provides the complete picture of the only present states of the system that are likely to be observed. The second condition holds almost surely, with respect to the measure $\mathbb{P}$, while the $B(\omega)$ are now random subsets of X; see [29] for further details.

The resulting random compact set $\bigcup_{\omega\in\Omega} \mathcal{A}(\omega)$ is called a *random attractor*; it is also called a *strong attractor* since the convergence of remote initial data to the attractor holds almost surely for the Hausdorff semi-metric of the phase space X [29,42–44]. Moreover, when $\{\theta_t\}$ is ergodic, then knowing $\bigcup_{t\in\mathbb{R}} \mathcal{A}(\theta_t\omega)$ yields $\bigcup_{\omega\in\Omega} \mathcal{A}(\omega)$, and vice versa. In other words, knowing the random attractor along one path ω yields all the possible states of the attractor at a given t.

RDS theory also provides a natural link between the forward and pullback approach. Pullback attraction involves convergence almost surely (see above) and it implies weak convergence forward, that is, convergence in probability only. A *weak attractor*, as opposed to the strong one above, is defined similarly, except that now one requires only that

$$\lim_{t\to\infty} d_X(\Phi(t, \omega)B(\omega), \mathcal{A}(\theta_t\omega)) = 0 \quad \text{in probability [42].}$$

A strong attractor is always a weak attractor, but the converse is obviously wrong [29,42]. The argument runs as follows: $\{\theta_t\}$ is measure-preserving and thus one has $\mathbb{P}\{\omega : \Phi(t, \omega)x \in D\} = \mathbb{P}\{\omega : \Phi(t, \theta_{-t}\omega)x \in D\}$, for any $x \in X$ and D any measurable subset of X. If the limit of the right-hand side exists as $t \to +\infty$, then the left-hand side converges as well; that is, $\Phi(t, \omega)x$ converges, but only in probability. There is a duality between fuzziness from the present into the future versus "determinism" from the past up to the present. This duality arises from the asymmetric way in which time is addressed in the RDS approach, through the concepts of *past and future of an RDS*; see Section 1.7 of [29].

3.3. Random invariant measures

So far, we have focused on the more appealing and intuitive aspects of RDS theory, with random attractors playing the key role. The fundamental objects in RDS theory, though, are in fact the random invariant measures; they are intimately linked to random attractors in forced dissipative systems.

When a global random attractor $\mathcal{A}$ exists, it supports all the invariant measures μ, and hence $\mu(\mathcal{A}) = 1$; this result is indeed similar to the deterministic situation. The invariant measures μ here are defined on the product space $\Omega \times X$ and invariance is with respect to the skew product Θ defined above, so that $\Theta(t)\mu = \mu$ for all t [29,34].

The invariant measures μ "lift" the probability measure $\mathbb{P}$, defined on Ω, into the extended phase space $\Omega \times X$, so that the

Please cite this article in press as: M.D. Chekroun, et al., Stochastic climate dynamics: Random attractors and time-dependent invariant measures, Physica D (2011), doi:10.1016/j.physd.2011.06.005

projection of μ on Ω equals $\mathbb{P}$. It is much more convenient, though, to work in the phase space X, rather than in the product space. Invariance of μ in X corresponds to the use of random measures $\omega \mapsto \mu_\omega$ on X called *sample measures* [32]; they are also known as *factorized or disintegrated measures* [29,34].

Under very general conditions, one can show there is a one-to-one correspondence between any μ_ω on X and any μ on the product space whose Ω-projection equals $\mathbb{P}$; symbolically $\mu(d\omega, d\mathbf{x}) = \mu_\omega(d\mathbf{x})\mathbb{P}(d\omega)$ [29]. In particular, to say that $\mu(\mathcal{A}) = 1$ is equivalent to $\mu_\omega(\mathcal{A}(\omega)) = 1$; i.e., each sample of $\mathcal{A}$ supports the sample measure μ_ω. The invariance of μ can now be written, since we take θ_t here to be invertible, as

$$\Phi(t, \omega)\mu_\omega = \mu_{\theta_t\omega}, \quad \text{almost surely with respect to } \mathbb{P}. \tag{4}$$

Note that the time-dependent solutions of the Fokker–Planck equation must not be confused with the time-dependent sample measures $\mu_{\theta_t\omega}$ discussed herein; see the discussion of Eq. (6) in Section 4.1 below. The main difference is apparent by returning now to question **Q**.

Indeed, the answer to our key question **Q** – at least when X is finite-dimensional – is simply that the regions where the stochastic flow ends up at time t – for a realization ω of the system's random aspects – may be determined by $\mathcal{A}(\omega)$ and distributed according to probabilities given by a specific invariant sample measure μ_ω. A condition for this to hold is the existence of a physical measure, i.e. an invariant measure which satisfies almost surely (with respect to $\mathbb{P}$) the key identity:

$$\lim_{t\to\infty} \frac{1}{t} \int_0^t G \circ \Phi(s, \theta_{-s}\omega)\mathbf{x}\, ds = \int_{\mathcal{A}(\omega)} G(\mathbf{x})\mu_\omega(d\mathbf{x}), \tag{5}$$

for almost every $\mathbf{x} \in X$ (in the Lebesgue sense), and for every continuous observable $G : X \to \mathbb{R}$. Eq. (5) is a direct generalization to the RDS framework of the concept of physical measure from the autonomous deterministic setting [2,14]. In the next section, we discuss a particular class of physical measures of interest, namely *random SRB measures*. These measures are a sample version of the classical SRB measures found in the autonomous context; see [32] and the next section here. We focus now on the simplest invariant measures that are fundamental in RDS theory.

Going back to the Langevin equation (3), since the random point $a(\omega) = \sigma \int_{-\infty}^0 \exp(\alpha\tau) dW_\tau(\omega)$ is the global random attractor of that system, we get that the random Dirac $\delta_{a(\omega)}$ supported by each point $a(\omega)$ is a globally stable invariant measure, which pullback attracts the Lebesgue measure of the real line. This result can be of course generalized to a higher-dimensional Langevin equation $d\mathbf{x} = L\mathbf{x} + d\mathbf{W}_t$, where L has good dissipative properties and where the random attractor $\mathcal{A}$ becomes the union of random vectors $\mathbf{a}(\omega)$ such that $\Phi(t, \omega)\mathbf{a}(\omega) = \mathbf{a}(\theta_t\omega)$ for all $t \geq 0$ and all $\omega \in \Omega$. For a more general RDS, a (measurable) random variable $\mathbf{a} : \Omega \to X$ is called a *random fixed point* of the system when this last equality holds. These random fixed points are the analogs of the steady states found in the autonomous setting.

When all the Lyapunov exponents are negative, then all the initial states are attracted to a single random fixed point. This well-known phenomenon occurs for general RDSs and is not restricted to linear dynamics with additive noise [45,46]; it is sometimes called *synchronization* [29,31]. When the random attractor is more complex than a random point, one may observe *intermittency*: for each realization ω, two arbitrary trajectories are either synchronized or not during variable time intervals. This on-off synchronization occurs exponentially fast; see Fig. 6 of [47]. It appears that the ENSO model studied below exhibits such intermittent behavior.

4. Numerical results and their RDS analysis

We consider in this section the Lorenz model [3] and the ENSO model of Timmerman and Jin (TJ hereafter) [40]. The two models have three degrees of freedom each and we perturb them by linearly multiplicative white noise [29] for the Lorenz model and by including white noise in a nonlinear term of the TJ model. Both models are low-dimensional truncations of sets of partial differential equations: the former of the classical Rayleigh–Bénard convection equations [48], and the latter of a coupled ocean–atmosphere model for ENSO due to Zebiak and Cane [49].

The deterministically chaotic regimes of these two models have very different power spectra: the Lorenz model exhibits a broad-band spectrum with exponential decay even in the low-frequency range [50], while the ENSO model we study in Section 4.3 below does exhibit LFV in its chaotic regimes [51]; the latter is characterized by a wide peak at low frequencies, which rises above a continuous background that has a power-law or exponential decay; see Appendix B and [52,53]. In both cases, we will illustrate how the sample SRB measures discussed in Section 3.3, and the RDS approach in general, allow us to differentiate these two types of chaos in the presence of noise.

4.1. A stochastically perturbed Lorenz model

In the deterministic context, geometric models were proposed in the 1970s [54] to interpret the dynamics observed numerically by Lorenz in [3]. These geometric models attracted considerable attention and it was shown that they possess a unique SRB measure [55,56], i.e., a time-independent measure that is invariant under the flow and has conditional measures on unstable manifolds that are absolutely continuous with respect to Lebesgue measure [2]. This result has been extended recently to the Lorenz flow [3] itself, in which the SRB measure is supported by a strange attractor of vanishing volume [57,58].

Even though this result was only proven recently, the existence of such an SRB measure was suspected for a long time and has motivated several numerical studies to compute a PDF associated with the Lorenz model [3], by filtering out the stable manifolds; e.g. [59,60] and references therein. The Lorenz attractor is then approximated by a two-dimensional manifold, called the *branched manifold* [54], which supports this PDF. Based on such a strategy, Dorfle and Graham [59] showed that the stationary solution of the Fokker–Planck equation for the Lorenz model [3] perturbed by additive white noise possesses a density with two components: the PDF of the deterministic system supported by the branched manifold plus a narrow Gaussian distribution transversal to that manifold.

It follows that, in the presence of additive noise, the resulting PDF looks very much like that of the unperturbed system, only slightly fuzzier: the noise smoothes the small-scale structures of the attractor. More generally, this smoothing appears in the forward approach – for a broad class of additive as well as multiplicative noise, in the sense of [29] – provided that the diffusion terms due to the stochastic components in the Fokker–Planck equation are sufficiently non-degenerate; see Appendix C.1. Hörmander's theorem guarantees that this is indeed the case for hypoelliptic SDEs [61]. The corresponding non-degeneracy conditions allow one to regularize the stationary solutions of the counterpart of the Fokker–Planck equation in the absence of noise, known as the transport equation,

$$\partial_t p(\mathbf{x}, t) = -\nabla \cdot (p(\mathbf{x}, \mathbf{t})\mathbf{F}(\mathbf{x})); \tag{6}$$

a measure-theoretic justification for this equation can be found, for instance in [62, p. 210].

Please cite this article in press as: M.D. Chekroun, et al., Stochastic climate dynamics: Random attractors and time-dependent invariant measures, Physica D (2011), doi:10.1016/j.physd.2011.06.005

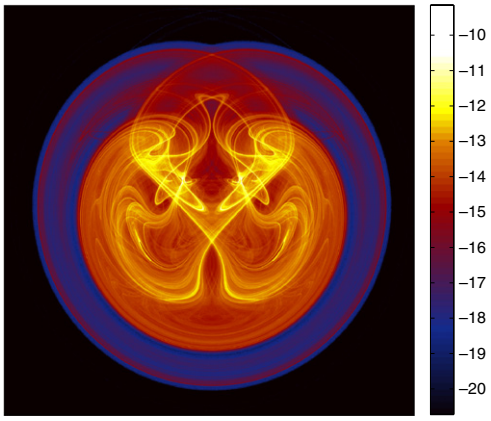

Fig. 1. Snapshot of the Lorenz [3] model's random attractor $\mathcal{A}(\omega)$ and of the corresponding sample measure μ_ω, for a given, fixed realization ω. The figure corresponds to projection onto the (y, z) plane, i.e. $\int \mu_\omega(x, y, z)dx$. One billion initial points have been used and the pullback attractor is computed for $t = 40$. The parameter values are the classical ones – $r = 28$, $s = 10$, and $b = 8/3$ – while $\sigma = 0.3$ and the time step $\Delta t = 5 \cdot 10^{-3}$. The color bar to the right is on a log-scale and quantifies the probability to end up in a particular region of phase space. Notice the interlaced filament structures between highly (yellow) and moderately (red) populated regions.

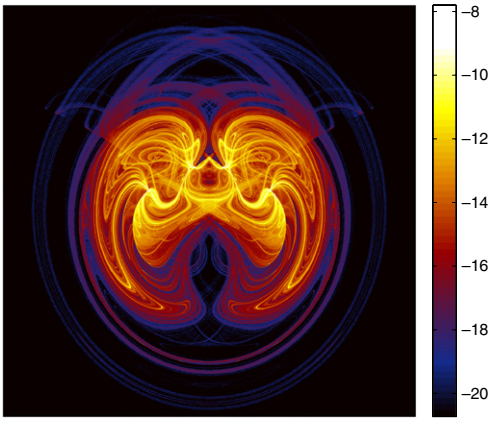

Fig. 2. Same as Fig. 1, for the same realization ω but with noise intensity $\sigma = 0.5$. Interlaced filament structures between highly and moderately populated regions are now much more complex. Weakly populated regions cover an important part of the random attractor and are, in turn, entangled with "zero-probability" regions (black).

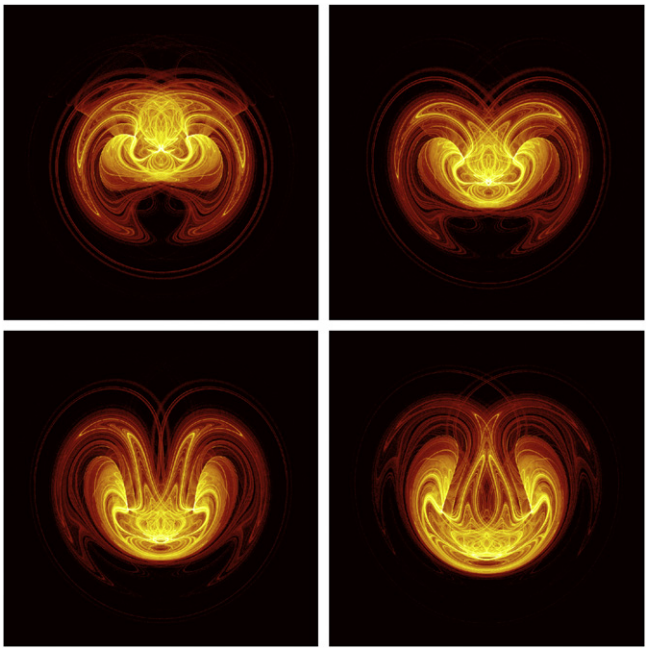

Fig. 3. Four snapshots of the random attractor and sample measure supported on it, for the same parameter values as in Fig. 2. The time interval δt between two successive snapshots – moving from left to right and top to bottom – is $\delta t = 0.0875$. Note that the support of the sample measure may change quite abruptly, from time to time; see the related short video in the SM for details.

This transport equation is also known as the Liouville equation and it provides the probability density at time t of $S(t)x$ when the initial state x is sampled from a probability measure that is absolutely continuous with respect to Lebesgue measure; here $\{S(t)\}_{t\in\mathbb{R}}$ is the flow of $\dot{\mathbf{x}} = \mathbf{F}(\mathbf{x})$, for some sufficiently smooth vector field $\mathbf{F}$ on $\mathbb{R}^d$. As a matter of fact, when $\mathbf{F}$ is dissipative and the dynamics associated with it is chaotic, the stationary solutions of (6) are very often singular with respect to Lebesgue measure; these solutions are therefore expected to be SRB measures. For a broad class of noises – such as those that obey a hypoellipticity condition – the forward approach leads us to suspect that noise effects tend to remove the singular aspects with respect to Lebesgue measure. This smoothing aspect of random perturbations is often useful in the theoretical understanding of any stochastic system, in particular in the analysis of the lower- and higher-order moments, which have been thoroughly studied in various contexts.

For chaotic systems subject to noise, however, this noise-induced smoothing observed in the forward approach compresses a lot of crucial information about the dynamics itself; quite to the contrary, the pullback approach brings this information into sharp focus. A quick look at Figs. 1–3 is already enlightening in this respect. All three figures refer to the invariant measure μ_ω supported by the random attractor of our stochastic Lorenz model **[SLM]**. This model obeys the following three SDEs:

$$[\mathbf{SLM}] \quad \begin{cases} dx = s(y - x)dt + \sigma x \, dW_t, \\ dy = (rx - y - xz)dt + \sigma y \, dW_t, \\ dz = (-bz + xy)dt + \sigma z \, dW_t. \end{cases} \tag{7}$$

In system (7), each of the three equations of the classical, deterministic model [3] is perturbed by linearly multiplicative noise in the Itô sense, with W_t a Wiener process and $\sigma > 0$ the noise intensity. The other parameter values are the standard ones for chaotic behavior [48], and are given in the caption of Fig. 1.

Figs. 1 and 2 show two snapshots of the sample measure μ_ω supported by the random attractor of **[SLM]** – for the same realization ω but for two different noise intensities, $\sigma = 0.3$ and 0.5, while Fig. 3 provides four successive snapshots of $\mu_{\theta_t\omega}$, for the same noise intensity as in Fig. 2, but with $t = t_0 + k\delta t$ and $k = 0, 1, 2, 3$ for some t_0.

The sample measures in these three figures, and in the associated short video given in the SM, exhibit amazing complexity, with fine, very intense filamentation; note logarithmic scale on color bars in the three figures. There is no fuzziness whatsoever in the topological structure of this filamentation, which evokes the Cantor-set foliation of the deterministic attractor [54]. Such a fine structure strongly suggests that these measures are supported by an object of vanishing volume.

Much more can be said, in fact, about these objects. RDS theory offers a rigorous way to define random versions of stable and unstable manifolds, via the Lyapunov spectrum, the Oseledec multiplicative theorem, and a random version of the Hartman–Grobman theorem [29]. These random invariant manifolds can support measures, like in the deterministic context. When the sample measures μ_ω of an RDS have absolutely continuous conditional measures on the random unstable manifolds, then μ_ω is called a *random SRB measure*.

Please cite this article in press as: M.D. Chekroun, et al., Stochastic climate dynamics: Random attractors and time-dependent invariant measures, Physica D (2011), doi:10.1016/j.physd.2011.06.005

We can prove rigorously, by relying on Theorem B of [32], that the sample measures of the discretized stochastic system obtained from the **[SLM]** model share the SRB property. Indeed, it can be shown that a *Hörmander hypoellipticity condition* is satisfied for our discretized **[SLM]** model, thus ensuring that the random process generated by this model has a smooth density $p(t, \mathbf{x})$ [63]; see Appendix C.1 for more details. Standard arguments [64] can then be used to prove that the stationary solution ρ of our model's Fokker–Planck equation is in fact absolutely continuous with respect to Lebesgue measure.

Since our simulations exhibit exactly one positive Lyapunov exponent, the absolute continuity of ρ implies that the sample measures seen in Figs. 1–3 are, actually, good numerical approximations of a genuine random SRB measure for our discretized **[SLM]**, whenever δt is sufficiently small; see also the next section. In fact, Ledrappier and Young's [32] Theorem B is a powerful result, which clearly shows that – in noisy systems, and subject to fairly general conditions – chaos can lead to invariant sample measures with the SRB property; we reformulate in Appendix C.2 this theorem in the present context. It is striking that the same noise-induced smoothing that was "hiding" the dynamics in the forward approach allows one here to exhibit the existence of an SRB measure from a pullback point of view, and thus to approximate the unstable manifolds supporting this invariant measure.

Note that since the sample measures associated with the discrete **[SLM]** system are SRB here, they are physical measures and can thus be computed at any time t by simply flowing a large set of initial data from the remote past $s \ll t$ up till t, for a fixed realization ω; this is exactly how Figs. 1–3 were obtained. Given the SRB property, the nonzero density supported on the model's unstable manifolds delineates numerically these manifolds; Figs. 1–3 provide therefore an approximation of the *global* random attractor of our stochastic Lorenz system.

Finally, these random measures are Markovian, in the sense that they are measurable with respect to the past σ-algebra of the noise [29]. The latter statement results directly from the fact that these measures are physical, cf. (5), and thus satisfy the required measurability conditions in the pullback limit. The information about the moments that is available in the classical Fokker–Planck approach is complemented here by information about the *pathwise moments*. These pathwise statistics are naturally associated with the sample measures – when the latter are SRB – by setting $\mathbf{G}(\mathbf{x}) := x_i^p, i = 1, 2, 3, p \in \mathbb{R}$ in Eq. (5), as we shall see in the next subsection.

The evolution of the sample measures $\mu_{\theta_t\omega}$ (see SM video) is quite complex, and two types of motion are present. First, a pervasive "jiggling" of the overall structure can be traced back to the roughness of the Wiener process W_t and to the multiplicative way it enters into the **[SLM]** model. Second, there is a smooth, regular low-frequency motion present in the evolution of the sample measures, which seems to be driven by the deterministic system's unstable limit cycles and is thus related to the well-known lobe dynamics. The latter motion is clearly illustrated in Fig. 3.

More generally, it is worth noting that this type of low-frequency motion seems to occur quite often in the evolution of the samples measures of chaotic systems perturbed by noise; it appears to be related to the recurrence properties of the unperturbed deterministic flow, especially when energetic oscillatory modes characterize the latter. The TJ model of ENSO is another example in which another type of low-frequency motion of the sample measures is present; see Fig. 7 in Section 4.3 below. To the best of our knowledge, there are no rigorous results on this type of phenomenon in RDS theory.

Besides this low-frequency motion, abrupt changes in the global structure occur from time to time, with the support of the sample measure either shrinking or expanding suddenly. These abrupt changes recur frequently in the video associated with Fig. 3, which reproduces a relatively short sequence out of a very long stochastic model integration; see the supplementary material (SM) in Appendix D.

As the noise intensity σ tends to zero, the sample-measure evolution slows down, and one recovers numerically the measure of the deterministic Lorenz system (not shown). This convergence as $\sigma \to 0$ may be related to the concept of *stochastic stability* [14,55]. Such a continuity property of the sample measures in the zero-noise limit does not, however, hold in general; it depends on properties of the noise, as well as of the unperturbed attractor [45,46,65].

As stated in the theoretical section, the forward approach is recovered by taking the expectation, $\mathbb{E}[\mu_\bullet] := \int_\Omega \mu_\omega \mathbb{P}(d\omega)$, of these invariant sample measures. In practice, $\mathbb{E}[\mu_\bullet]$ is closely related to ensemble or time averages that typically yield the previously mentioned PDFs. In addition, when the random invariant measures are Markovian and the Fokker–Planck equation possesses stationary solutions, $\mathbb{E}[\mu_\bullet] = \rho$, where ρ is such a solution. Subject to these conditions, there is even a one-to-one correspondence between Markovian invariant measures and stationary measures of the Markov semigroup [29,34]. The inverse operation of $\mu \mapsto \rho = \mathbb{E}[\mu_\bullet]$ is then given by $\rho \mapsto \mu_\omega = \lim_{t\to\infty} \Phi(-t, \omega)^{-1}\rho$; the latter is in fact the pullback limit of ρ due to the cocycle property [34]. It follows readily from this result that RDS theory "sees" many more invariant measures than those given by the Markov semigroup approach: non-Markovian measures appear to play an important role in stochastic bifurcation theory [29], for instance.

To summarize, one might say that the classical forward approach considers only expectations and PDFs, whereas the RDS approach "slices" the statistics very finely: the former takes a hammer to the problem, while the latter takes a scalpel. Clearly, distinct physical processes may lead to the same observed PDF: the RDS approach and, in particular, the pullback limit are able to discriminate between these processes and thus provide further insight into them.

4.2. Numerical stability of the sample measures

In this subsection, we perform simple numerical tests on the stability of the sample measures μ_ω computed in the previous subsection. We keep the same parameter values as in Fig. 2 and perturb slightly the noise intensity σ from its value $\sigma_0 = 0.5$.

Let C be a fixed cube in $\mathbb{R}^3$ such that the support of the measures always lies in C. We discretize C over a regular mesh with N^3 nodes and obtain a brute-force numerical approximation $\mu_\omega^{\sigma_0,N}$ of the measures $\mu_\omega^{\sigma_0}$ by simply flowing an ensemble of initial data of size n with the stochastic flow of our **[SLM]**, over a long time interval. This large ensemble is uniformly distributed on the given N-partition of C and the noise realization ω is fixed. Since the results in Section 4.1 allow us to prove that any discrete, and numerically stable, approximation of our **[SLM]** possesses a sample SRB measure, it follows that $\mu_\omega^{\sigma_0}$ is a physical measure that answers the question **Q** of Section 2.2, and therefore it attracts the Lebesgue measure on C. The SRB property strongly suggests that $\mu_\omega^{\sigma_0,N}$ provides a good approximation of the sample SRB measures of the discretized **[SLM]**, as n and N increase, although a rigorous convergence analysis would be necessary to corroborate this intuition. This property also indicates that the nature of the distribution of initial states is not important, provided this distribution is absolutely continuous with respect to the Lebesgue measure.

In the deterministic context, the road for a rigorous analysis has been paved over the past decades. The underlying methods are

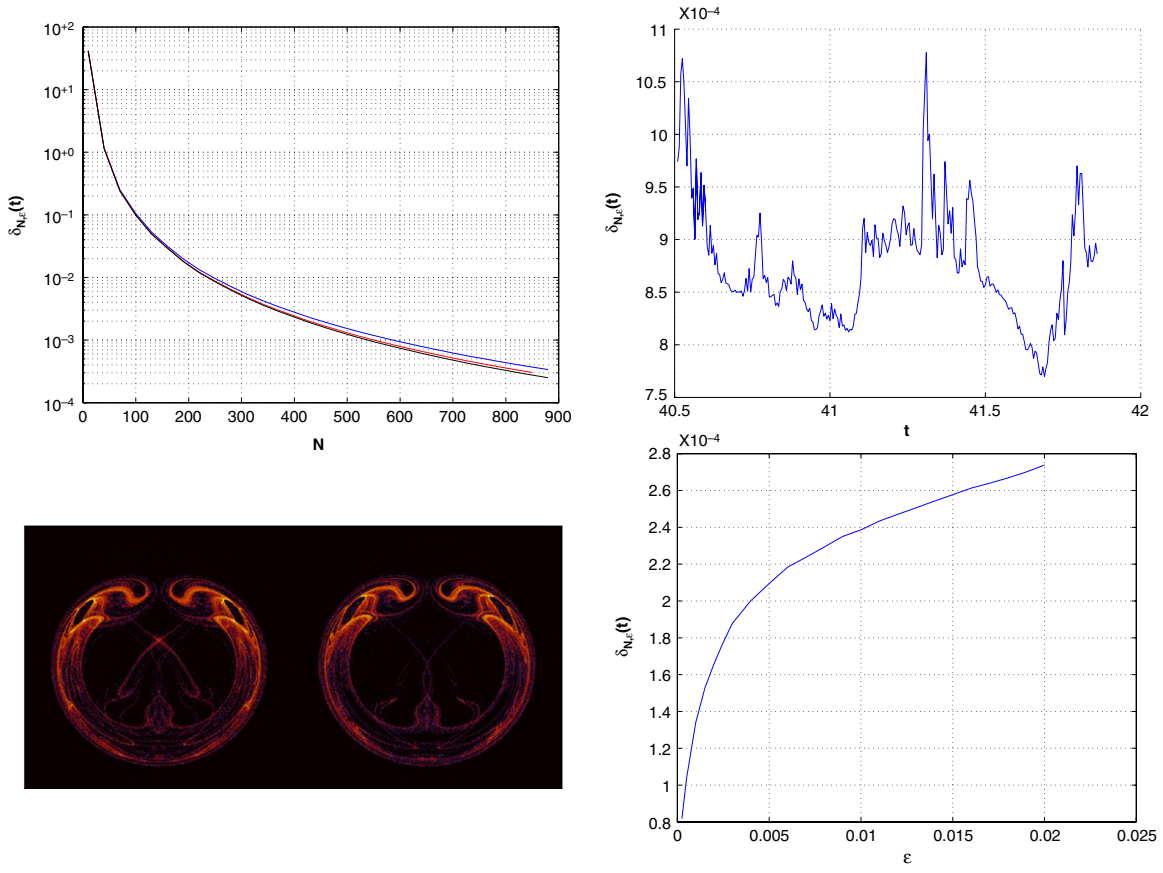

Fig. 4. Numerical stability of the invariant sample measures of Fig. 2. The upper-left panel shows the L_1-error $\delta_{N,\epsilon}(t)$ as a function of N for $\epsilon = 10^{-2}$ and three different sets of initial data; the number of points n in the latter is $n = 50^3$, 100^3 and 300^3 for the blue, red and black curves, respectively. The upper-right panel displays $\delta_{N,\epsilon}(t)$ for t varying over 1.5 time units, $40.5 < t < 42.0$, while $N = 600$ and $\epsilon = 10^{-2}$. The lower-left panel plots a snapshot of the two sample measures that correspond to noise intensity σ_0 and $\sigma_0 - \epsilon$ at the end of the time series of $\delta_{N,\epsilon}(t)$ in the upper-right panel. The lower-right panel shows $\delta_{N,\epsilon}(t)$ as a function of ϵ for $N = 900$ and $n = 200^3$; this error clearly converges to zero as $\epsilon \to 0$.

essentially based on a time-dependent matrix approximation $\hat{P}_t^N$ over the N-partition of the infinite-dimensional *Perron–Frobenius* or *transfer operator* P_t, where P_t is naturally associated with the semigroup induced by the transport equation (6) [66]. It is the fixed points of this operator that give the invariant measures; e.g. [62,67–70] and references therein. These methods are rooted in Ulam's method [71] and SRB measures have been typically obtained as a weak limit of the densities of Markov chains governed by $\{\hat{P}_t^N\}$, as $N \to \infty$. Using a directed-graph representation of the partition, Osipenko [72] has proposed an alternative approach that also allows one to rigorously approximate certain invariant measures – which are not necessarily SRB but are ergodic, and thus still physically interesting – by flows on this graph.

Similar approaches can be extended to a nonautonomous, as well as a random setting, by considering the Perron–Frobenius operator obtained essentially by inversion of (4) [73]. Froyland et al. [74] and Dellnitz et al. [70] have thus computed eigenvectors of the approximating matrices $\hat{P}_t^N$ that correspond to eigenvalues close to 1 in the nonautonomous context, and Julitz [73] has computed random attractors by using an extension of the subdivision algorithm [75,76] in a stochastic context. Still, much remains to be done for the computation of sample SRB measures in the RDS setting.

Given the scope of the present article, it appeared sufficient for our purposes to adopt a brute-force approach to the numerical calculations for the **[SLM]** model in Section 4.1. This approach still allows us to perform a sensitivity analysis of the numerical results so obtained. We thus consider the L^1-error $\delta_{N,\epsilon}(t) := \int_C |p^{\sigma_0,N}_{\theta_t\omega} - p^{\sigma_0-\epsilon,N}_{\theta_t\omega}|\, d\mathbf{x}$, where $p^{\sigma,N}_{\theta_t\omega}(\mathbf{x})$ is the "probability density" of the discrete sample measure $\mu^{\sigma_0,N}_{\theta_t\omega}$ and the integral is evaluated on the N^3-mesh.

The upper-left panel of Fig. 4 shows the dependence of $\delta_{N,\epsilon}(t)$ with respect to N for fixed t and $\epsilon = 10^{-2}$, and for three different sets of initial data, with an increasing number n of points (see caption). There is very little difference between the three curves, indicating that the number n is already large enough to guard against sampling error. An error of less than 1% is achieved for meshes of size $200 \leq N \leq 900$. The brute-force estimate of sensitivity given by the L^1-norm is thus not subject to quantization effects in the number of initial data, provided that n is sufficiently large.

The evolution of $\delta_{N,\epsilon}(t)$ for the same ϵ and $N = 600$ is plotted in the upper-right panel of Fig. 4. This plot indicates that, as the sample measures evolves with θ_t, they remain close to each other for all time; here $7.5 \cdot 10^{-4} \leq \delta_{N,\epsilon}(t) \leq 11 \cdot 10^{-4}$.

The lower-left panel shows an actual snapshot of the two measures at a fixed time t, at the end of the time series plotted in the upper-right panel, for $N = 900$ and $\epsilon = 10^{-2}$. Only tiny differences become visible when zooming in on the electronic file of the figure (see SM). As a matter of fact, for $\epsilon < 10^{-3}$, the two measures are no longer distinguishable by eye for the N used. This visual similarity between $\mu^{\sigma_0,N}_{\omega}$ and $\mu^{\sigma_0-\epsilon,N}_{\omega}$ for $N = 900$ is in excellent agreement with the error of less than 0.1% in the L^1-difference.

The error $\delta_{N,\epsilon}(t)$ is plotted in the lower-right panel as a function of ϵ, demonstrating clearly that the function $\epsilon \mapsto \mu^{\sigma_0-\epsilon,N}_{\omega}$ is

L^1-continuous at $\epsilon = 0$, since the difference between the two measures tends to zero in L^1 as $\epsilon \to 0$. This result, moreover, is independent of the noise intensity σ_0 (not shown).

From the SRB property and Eq. (5), we thus conclude that, for almost all realizations, any observable of our discretized **[SLM]** depends continuously on the noise intensity and, in particular, on the pathwise moments of the components of **[SLM]**, by setting $\mathbf{G}(\mathbf{x}) := x_i^p$, $i = 1, 2, 3$, $p \in \mathbb{R}$ in Eq. (5). We will refer to the latter property as *pathwise statistical stability* of our **[SLM]**.

We conclude that the numerical results shown in this paper are very robust. Note that we cannot precisely estimate the level of accuracy with which the sample measures are computed, although the results of this subsection indicate they are quite good, due to the very large ensembles of initial states we used. Unfortunately, statistical methods for improving PDF estimates, like kernel density estimation, require densities that are at least twice differentiable, while the numerical evidence here is that the sample measures of our stochastic system are strongly suspect of not being even absolutely continuous with respect to Lebesgue measure; in particular, they are not differentiable even once.

4.3. A stochastic ENSO model and its RDS analysis

In this subsection, we compute the stochastic TJ model's sample measures to obtain more detailed information on this model [40,51]. These sample measures enable us to understand at a deeper level the interaction between noise and nonlinearity in this slightly more realistic climate model. Our theoretical laboratory is climate variability in the Tropical Pacific, which is characterized by the interannual ENSO oscillation. A variety of modeling studies and observations strongly suggest that the irregular, 2–7-year time scale of ENSO is produced by nonlinear ocean–atmosphere interactions in this region [27,28]. In addition, this variability is bracketed by high-frequency, intraseasonal noise due to so-called "westerly wind bursts" in the surface winds, and by interdecadal changes in the global ocean circulation [38].

Aside from global effects that act on interdecadal time scales, these time scales may also arise from the interaction between noise and purely tropical effects [77]. Timmermann and Jin [40] argued, based on a dynamical analysis of the Jin model [33], that long-term changes in ENSO activity may result from perturbations of a homoclinic orbit specifically associated with the nonlinear advection terms in the model's sea surface temperature equation. Using the classical forward approach, they noted that such conclusions are robust against the introduction of wind-generated noise in the model.

For the sake of completeness and consistency, we describe here briefly the low-order, coupled model of tropical atmosphere–ocean interactions [33,40,51] that we use. This model can be derived from a simplified version of Zebiak and Cane's ENSO model [49] by using a two-strip-and-two-box approximation [33]. By assuming symmetry with respect to the equator, the model focuses on changes across one equatorial and one off-equatorial strip [33]. The upper ocean is a two-box version of a shallow-water model for the equatorial ocean, combined with a mixed layer of fixed depth [49]; the two boxes are the western (135°E–155°W) and the eastern equatorial region (155°–85°W) [78]. The ocean–atmosphere interaction is approximated by a linear relationship between surface winds and the sea surface temperature (SST) gradient.

The reduced model has three variables: the SSTs T_1 and T_2 in the western and eastern Tropical Pacific, respectively, and the depth anomaly h of the western equatorial thermocline [33,40,51]. Their evolution is governed by a stochastic system composed of three prognostic (i.e., differential) equations, coupled with two diagnostic (i.e., algebraic) equations:

$$\textbf{[STJ]}\quad \begin{cases} \dot{T}_1 = -\alpha(T_1 - T_r) - (2\epsilon u/L)(T_2 - T_1), \\ \dot{T}_2 = -\alpha(T_2 - T_r) - \dfrac{w}{H_m}(T_2 - T_{\mathrm{sub}}(h)), \\ \dot{h} = r(-h - \dfrac{bL}{2}\mathfrak{T}(T_1, T_2)), \\ T_{\mathrm{sub}}(h) = T_r - \left(\dfrac{1}{2}(T_r - T_{r0})\right) \\ \qquad \times \left(1 - \dfrac{1}{h^*}\tanh\Big(H + bL\cdot\mathfrak{T}(T_1, T_2) + h - z_0\Big)\right) \\ \mathfrak{T}(T_1, T_2) = \dfrac{a}{\beta}(T_1 - T_2)(\xi_t - 1). \end{cases} \tag{8}$$

The wind-stress anomalies $\mathfrak{T}$ in the last equation of (8) are assumed to depend on the western and eastern SSTs, $\mathfrak{T} = \mathfrak{T}(T_1, T_2)$, and the zonal advection is given by $u = \beta L\mathfrak{T}(T_1, T_2)/2$. In the eastern Tropical Pacific, the equatorial upwelling is given by $w = -\beta\mathfrak{T}(T_1, T_2)/H_m$, while $T_{\mathrm{sub}} = T_{\mathrm{sub}}(h)$ there represents the subsurface temperature and has a saturation effect on the dynamics; thermal relaxation toward a radiative–convective equilibrium temperature T_r is assumed in modeling T_{sub}. Wind-stress bursts are parameterized as white noise ξ_t of variance σ, while ϵ measures the strength of the zonal advection and serves as a bifurcation parameter in the model [40,51]. We refer to [40] for other subsidiary variables and for a table of parameters used in the numerical results obtained hereafter.

The TJ model [33,40] is not only closer in its physical derivation to global climate dynamics than the stochastic Lorenz model **[SLM]**, but it also exhibits LFV [51], which is an important ingredient of climate variability but is not present in the latter [15,79]. We are also interested in the TJ model because the way in which the noise enters into the Eqs. (8) makes it difficult to guess its effects on the deterministic dynamics. Does the model exhibit noise-induced Hopf bifurcation or more complicated, noise-sustained oscillation scenarios, and how would either of these alternatives affect our understanding and prediction of ENSO variability [15,39,79]?

Our aim here is to show that a pullback approach based on physical sample measures is better suited for the study and rigorous interpretation of stochastic effects on climatic LFV than using merely a forward, PDF-type approach. The pullback approach can even provide interesting information that complements standard power spectrum analysis. We believe that these statements are likely to be true for any problem involving both noise and chaotic behavior associated with LFV.

We show first that the deterministic version of the **[STJ]** model, with the noise turned off, exhibits – as the strength of the zonal advection ϵ increases – sharp transitions between distinct regimes with complex dynamics. These transitions include Hopf bifurcations, as well as chaotic behavior associated with so-called *single-pulse homoclinic orbits* that arise from a Shil'nikov-type bifurcation [80]. The associated qualitative jumps are clearly apparent in the left panel of Fig. 5, as the system's power spectrum changes with ϵ. When the noise is turned back on, we see in the right panel of Fig. 5 that these qualitative changes are completely smoothed out. This smoothing interferes with a reliable dynamical interpretation regarding the origin of the LFV exhibited by the **[STJ]** model in its chaotic regimes. As we shall see forthwith, the pullback approach does provide sharper insights into this LFV.

Recall that, if the deterministic model's variability is damped, adding even small-amplitude stochastic forcing can easily result in significant nonlinear effects; see [38,39] and references therein. Such a noise-induced excitation of supercritical behavior at deterministically subcritical parameter values does indeed occur in our numerical study of the **[STJ]** model. We were able to confirm

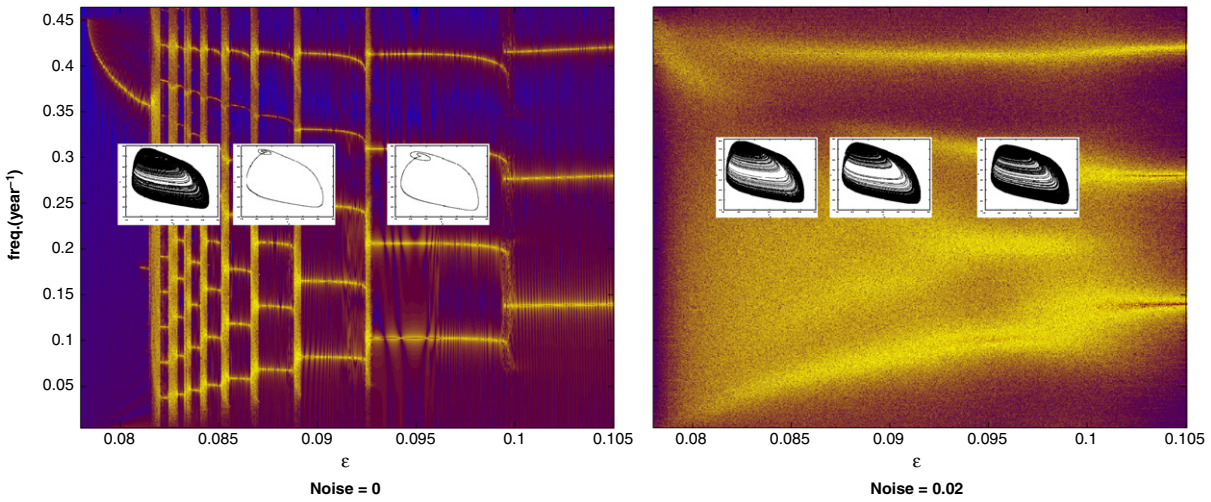

Fig. 5. Power spectrum of the **[STJ]** model as a function of the control parameter ϵ: (left panel) deterministic *versus* (right panel) stochastic. The color bar (not shown) is on a logarithmic scale. Sharp transitions between different types of quasi-periodic and chaotic behavior are apparent in the left panel, for zero noise; note the presence of windows of stability with one attracting limit cycle. Several model trajectories are, in fact, displayed; they include Shil'nikov-type orbits in the left panel as well. The sharp transitions in the left panel are completely smoothed out in the right panel, and the homoclinic orbits disappear, too; see also discussion in Section 4.2.

the presence of a Shil'nikov-type bifurcation to homoclinic orbits in the deterministic model, and show that the noise helps trigger horseshoe-like behavior in phase space for parameter ranges in which the deterministic model has only a stable limit cycle or even a stable steady state. All these noise-induced phenomena possess geometric features captured by the random attractors; see Fig. 6.

For instance – in the damped regime, with the right amount of noise – the global random attractor $\mathcal{A}(\theta_t\omega)$ of our **[STJ]** model is a closed curve, whose length and location in phase space vary with time, i.e., a random periodic orbit [81] that pullback attracts the Lebesgue measure of the phase space. This *random limit cycle* is associated with a broad spectral peak (not shown). One can thus observe here how the pullback approach provides a clearer dynamical perspective on the origin of the **[STJ]** model's LFV.

We proceed to study next the **[STJ]** model in a chaotic regime, i.e. when zonal advection is sufficiently strong. In the absence of noise (not shown), the model does exhibit interdecadal variability. This variability is due to the nearby presence in parameter space of a homoclinic orbit, whose characteristic amplitude modulation can be seen in the time series of T_2; see upper-left panel of Fig. 7. When including the noise that models wind-stress bursts, the sample measures shown in this figure's other panels still possess a complex structure.

The six sample measures $\mu_{\theta_t\omega}$ shown in the bottom panels of Fig. 7, at interannual intervals of $\delta t = 1.6$ years, are even more obviously singular than those in Figs. 1–4: at every time t, the regions that are most populated by the stochastic flow are confined mainly to filaments near the sharp peak (white + sign) that is located in the upper-left corner of the $(h - T_2)$ plane. For the decadal time scale of $6 \times 1.6 \simeq 10$ years, the change in probability of occurrence of El Niño episodes, with warm T_2, is clearly visible, while the spectral signature of the underlying random attractor may be undistinguishable from that of the random limit cycle.

The distinction in solution behavior between the two stems from the intermittency [47] that our **[STJ]** model exhibits in the chaotic regime; this intermittency is clearly visible in the T_2 time series in the upper-left panel of Fig. 7. The model's intermittency seems to be related to the structure of its random attractor, which differs from that of the **[SLM]** model shown in Figs. 1–3. The intermittency of the **[STJ]** model is that of noisy relaxation oscillators, as already documented for the noisy Duffing–Van der Pol oscillator. The random attractor of the latter is – in certain chaotic regimes – even more singular than that seen in Figs. 6 and 7 here [47]. This singular character is due to the random attractor's "nearly zero-dimensional" geometry, in the sense that its sample SRB measure is highly concentrated in a small neighborhood of one point of the phase space, with a small additional fraction supported by thin filaments that meander in-and-out of this neighborhood. Fig. 7 strongly suggests that our **[STJ]** model's behavior lies in between a random point – as observed in certain ENSO models that are governed by linear dynamics with additive noise (e.g., [82]) – and a noisy chaotic model with strong mixing, like **[SLM]**; see Appendix A for a precise definition of random dynamical systems that exhibit strong mixing.

In a more general context, the relationships noticed here between intermittent behavior and the nearly zero-dimensional geometry of the sample SRB measures seem to be associated with the single-pulse homoclinic orbits also present in relaxation oscillations [80]. This conjecture needs, however, to be further clarified, both physically and mathematically: the extent to which a system exhibiting LFV does present pathwise intermittency with sample SRB measures of nearly vanishing dimension requires proper investigation. In the case of our **[SLM]** model, for example, the spectrum is exponentially decaying [50,79], whereas the **[STJ]** model studied here does exhibit a broad peak in its power spectrum, with significant oscillatory modes still present in the chaotic regime illustrated in Fig. 7. Interestingly, the random attractors of the two models are quite different in their spatio-temporal phase-space patterns.

In fact, certain consequences of the nearly zero-dimensional aspect of a sample SRB measure possessing a sharp peak can be fairly well understood. This is the case regarding the dependence on initial state for a fixed realization ω. Indeed, the existence of regions with very low probability is an obvious corollary of such "peaky" sample measures, and it implies that almost all initial data are synchronized by the noise.

This synchronization leads naturally to a weak dependence on initial data, at least on sufficiently long time scales, namely of order greater than the system's characteristic dissipation time. The **[STJ]** model does exhibits such a weak dependence, whereas the **[SLM]** model does not. More generally, it seems important to note that these two systems have very different mixing properties [83] and decay of correlations: exponential in the **[SLM]** case and subexponential in the **[STJ]** case. The latter assertion relies, so far,

Please cite this article in press as: M.D. Chekroun, et al., Stochastic climate dynamics: Random attractors and time-dependent invariant measures, Physica D (2011), doi:10.1016/j.physd.2011.06.005

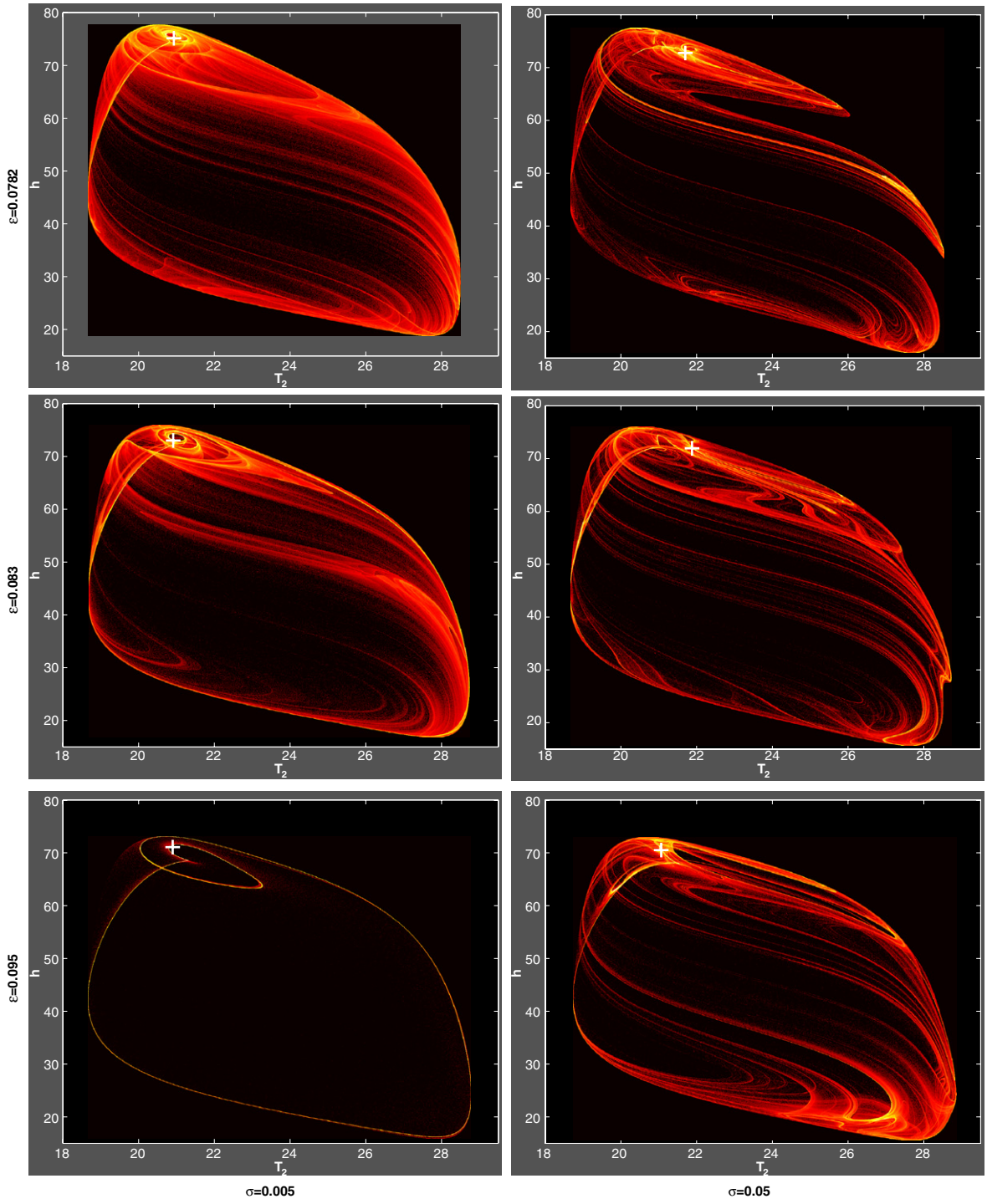

Fig. 6. Sample measures of the **[STJ]** model as a function of the control parameter ϵ and the noise intensity σ. The corresponding deterministic regimes, at $\sigma = 0$, are: $\epsilon = 0.0782$, a stable fixed point; $\epsilon = 0.083$, a homoclinic trajectory; and $\epsilon = 0.095$, a twisted limit cycle. Same qualitative color bar as in Figs. 1–3: highly populated regions in yellow, moderately populated in red, and near-zero population in black (logarithmic scale). These sample measures supported on the model's attractor reveal interesting noise-induced scenarios that are difficult to deduce in the forward approach. We thus see, at ($\epsilon = 0.0782$, $\sigma = 0.005$), that horseshoe-like behavior in phase space can be noise excited even for ϵ-values for which the deterministic dynamics exhibits an attracting fixed point, provided the noise is sufficiently strong.

only on numerical evidence: rigorous justification is quite a bit harder to obtain; see [83] and references therein for a survey.

To summarize, the **[STJ]** model possesses two main types of random attractor: (i) a random limit cycle in the deterministically damped regime; and (ii) a random attractor associated with intermittency in chaotic regimes. The first one may be of interest in understanding certain features that are displayed by fairly realistic models of the tropical ocean driven by surface winds [39], while the second one needs further investigation, theoretically as well as practically. Both offer new perspectives in the understanding of ENSO variability, as well as of other climate systems that exhibit LFV [5,15,84].

5. Concluding remarks

We have briefly motivated and outlined the main concepts and tools of RDS theory, in particular how to rigorously define

Please cite this article in press as: M.D. Chekroun, et al., Stochastic climate dynamics: Random attractors and time-dependent invariant measures, Physica D (2011), doi:10.1016/j.physd.2011.06.005

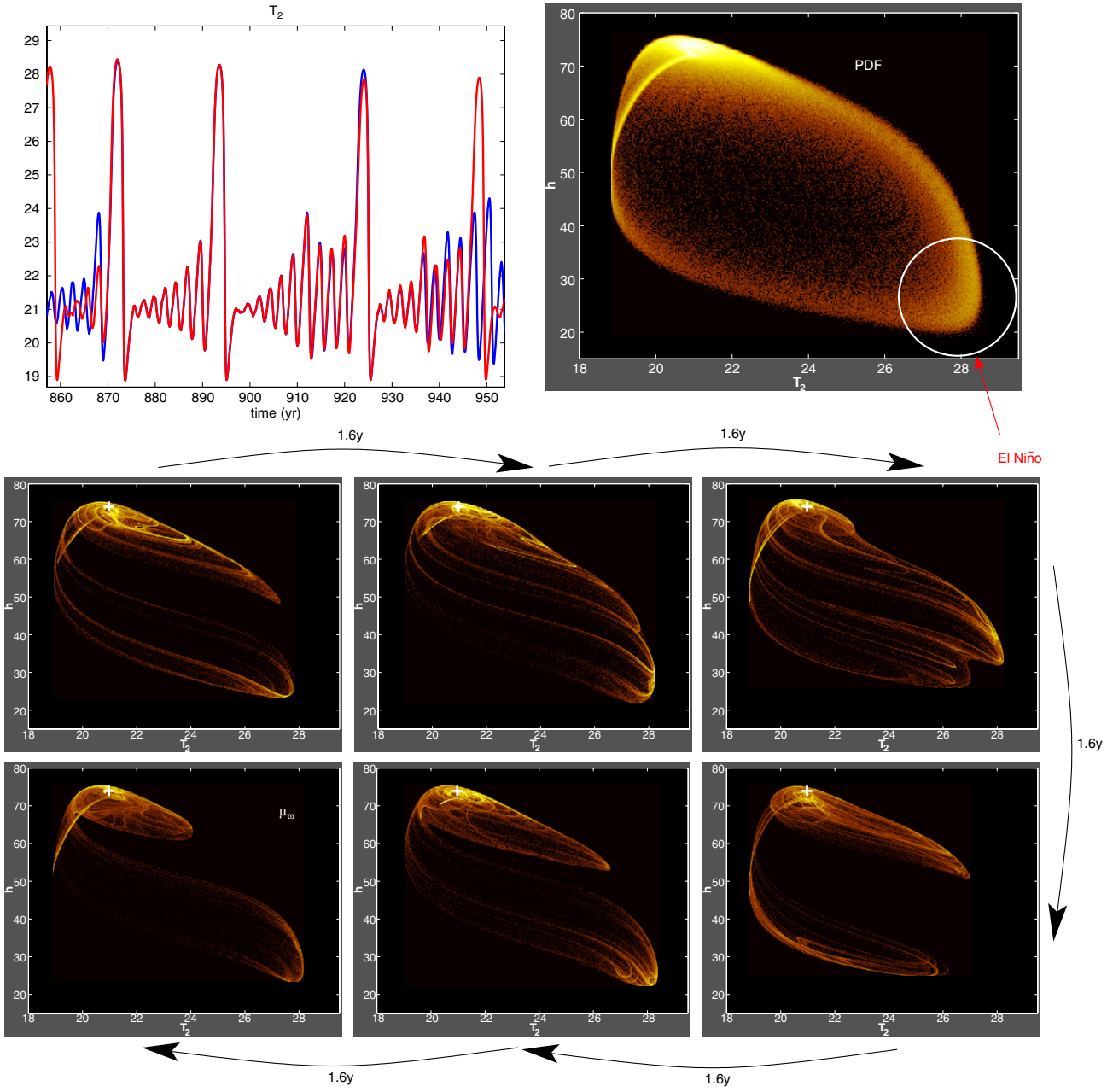

Fig. 7. Evolution of **[STJ]** model behavior in time, for $\epsilon = 0.0782$ and $\sigma = 0.005$. Intermittency is illustrated in the upper-left panel, for two different initial states at $t = 0$ (blue and red curves; time in years on the abscissa) and the same realization ω; where the two curves are visually indistinguishable, only the red curve appears. The forward PDF is shown in the upper-right panel: it averages the sample measures μ_ω. Six snapshots of the latter are shown at regular, 1.6-year intervals in the bottom panels; they are projected onto the $(h - T_2)$ plane, with T_2 on the abscissa, and their timing corresponds to the interannual variability of a long ENSO cycle.

stochastic flows and random attractors, as well as the corresponding invariant random measures. It appears from this outline that a stochastically perturbed system's pullback, strong attractor [42] provides much more detailed information on the system's dynamics and statistics than its PDF alone.

Detailed computations of the invariant sample measures for the stochastic Lorenz model **[SLM]** reveal the amazing complexity that underlies its PDF; see Figs. 1–3. The numerical results were shown to be quite robust (Fig. 4) and suggest that the actual measures are Markovian random SRB measures [14] associated with one positive Lyapunov exponent.

We saw, moreover, that other noisy systems with a positive Lyapunov exponent possess random attractors, which – while exhibiting a less striking geometry – still support nontrivial sample measures (Figs. 5 and 6) and are associated with intermittent synchronization. This type of behavior was illustrated on hand of the nonlinear stochastic ENSO model **[STJ]** of [40]. We showed in Fig. 7 that the sample-measure's evolution in time conveys information that greatly facilitates the physical interpretation of the dynamics.

On a longer, multidecadal time scale, the RDS approach could be combined with linear response theory [85]. When noise is absent, the fact that the physical invariant measure is absolutely continuous only along the unstable manifold implies that the fluctuation–dissipation theorem (FDT) cannot be applied in its classical form [86,87]. For hyperbolic deterministic systems, precise estimates exist for the response of their SRB measures to perturbations [85,88]. Based on this framework, the response to deterministic perturbations has been studied in [18–22] in a climatic context; climate response to stochastic perturbations should be

Please cite this article in press as: M.D. Chekroun, et al., Stochastic climate dynamics: Random attractors and time-dependent invariant measures, Physica D (2011), doi:10.1016/j.physd.2011.06.005

next and may provide more robust climate projections than available so far [7,31]. A mathematically rigorous justification of linear response theory for forced dissipative stochastic dynamical systems has been developed recently in [89]. The results of [89] support the experimental fact that for good systems, the mathematical formulation of FDT as linear response theory applies when the expectation of the μ_ω's (or its ergodic equivalent obtained by averaging over time for a single noise realization) is considered. The good systems are here the hypoelliptic ones where the improved regularity due to the presence of noise – in a forward sense (cf. Appendix C.1) – simplifies key aspects of the problem of a rigorous justification of linear response theory and circumvents the difficulties found to occur even in relatively simple deterministic systems [85]. Based on the established results for deterministic SRB measures [85], it appears feasible to extend rigorously linear response theory to SRB sample measures, at least for random hyperbolic systems [90]. Note that the pullback approach may combine furthermore a deterministic time-dependent forcing with a stochastic one. To do so, it suffices to work with the appropriate skew product and the relevant driving systems: one associated with the deterministic time-dependent forcing and one with the stochastic one; see e.g. [91]. This general abstract framework offers a natural ground for a mathematical formulation of FDT as linear response theory for time-dependent stochastic systems of interest in climate change science [31].

Moving on to intermediate models, the numerical results of [92] – using a so-called hybrid coupled model that couples an empirical, diagnostic atmosphere to an oceanic GCM [15,36] – showed that noise can shift as well as broaden the model's spectral peaks (see Figs. 6 and 8 there). Here again, the RDS approach could provide deeper insights into this phenomenon.

A key question arises of course, as it did for many novel mathematical concepts and tools, when first applied in the climatic or, more generally, physical context. The question is how to extend these novel ideas to more detailed and realistic models and even to observational data sets [15,84]. This question is under investigation for certain intermediate ENSO models and results will be reported elsewhere; see however [96] for an illustration of the pathwise approach in prediction of ENSO by a model of intermediate complexity.

Acknowledgments

We are grateful for discussions and encouragement to D. Kondrashov, J.C. McWilliams, J.D. Neelin, and I. Zaliapin. Two anonymous referees and V. Lucarini provided constructive and insightful comments. This study was supported by DOE grants DE-FG02-07ER64439 and DE-FG02-02ER63413 and by NSF grant DMS-1049253.

Appendix A. Mixing in random dynamical systems

In this appendix, we define rigorously the concept of an ω-wise mixing RDS, in the continuous-time context. Recall first the well-known definition of mixing in a deterministic dynamical system. Given a flow $\{\phi_t\}$ on a topological space X, which possesses an invariant (Borel) probability measure μ, we say that the dynamical system (ϕ_t, μ) is mixing if for any two measurable sets A and B,

$$\mu(A \cap \phi_{-t}(B)) \underset{t\to\infty}{\longrightarrow} \mu(A)\mu(B), \tag{9}$$

or equivalently,

$$\int F \cdot (G \circ \phi_t) d\mu \underset{t\to\infty}{\longrightarrow} \int F d\mu \int G d\mu, \tag{10}$$

for any pair of continuous functions $F, G : X \to \mathbb{R}$. Eq. (9) states that the set of points in A whose images belong to B by $\{\phi_t\}$ tends toward having the same proportion in A as B has in X, with proportions being understood in terms of the measure μ. Hence any measurable set will tend to redistribute itself over the state space according to μ.

Let us now consider a cocycle $\{\Phi(t,\omega)\}_{(t,\omega)\in\mathbb{R}\times\Omega}$ on the base space $(\Omega, \mathcal{F}, \mathbb{P}, \{\theta_t\})$, which possesses the sample measures $\{\mu_\omega\}$. We say that Φ is *ω-wise mixing* or *fiber mixing* [93] – or even simply mixing, if no confusion is possible – if for any random sets [43] $A(\omega)$ and $B(\omega)$,

$$\mu_\omega\Big(A(\omega) \cap \Phi(t,\omega)^{-1}\big(B(\theta_t\omega)\big)\Big) \underset{t\to\infty}{\longrightarrow} \mu_\omega(A(\omega))\mu_{\theta_t\omega}(B(\theta_t\omega)), \tag{11}$$

almost surely with respect to $\mathbb{P}$. This mixing concept and its interpretation are natural extensions of their deterministic counterparts just recalled above, except that the mixing property has to be checked across the fibers ω and $\theta_t\omega$, due to the skew-product nature of the RDS (Φ, θ) [93].

Appendix B. Low-frequency variability (LFV) and mixing

Low-frequency variability (LFV) is a widely used, but not clearly defined concept in the atmospheric, oceanic and climate sciences [48,15,31]. In general, one just refers to phenomena whose periods are longer than those previously studied. Examples include atmospheric LFV – referring to so-called intraseasonal oscillations whose characteristic time scale of 10–100 days is longer than the 5–10-day life cycle of mid-latitude storms but not longer than a season [15,84] – or oceanic LFV referring to interannual or interdecadal variability whose characteristic time scales are longer than the several-months-long ones of mesoscale eddies and the seasonal cycle of a year [5,15].

In this appendix, we clarify the notion of LFV from a mathematical perspective. Let us reconsider the deterministic Lorenz system [3]. It is known that the power spectral density, or power spectrum, of this system is exponentially decaying [50,79]. At the same time, one can check numerically that the decay of the autocorrelation function is exponentially decaying, too. Other types of power spectrum behavior may be encountered for chaotic dynamical systems, though. Aside from pure power-law decay, it may also happen that the power spectrum contains one or several broad peaks that stand out above the continuous background, whether the latter has a power-law [53] or exponential decay. If the central frequencies of these peaks are located in a frequency band that lies close to the lower end of the frequency range being studied, the system is said to exhibit LFV [52,79].

This climatically motivated, but vague notion of LFV can be tentatively formalized mathematically through the mixing concept introduced in Appendix A. Indeed, for a general flow $\{\phi_t\}$ on a topological space X, which possesses an invariant physical measure μ, let us define the correlation function by

$$C_t(F,G) := \left| \int F \cdot (G \circ \phi_t) d\mu - \int F d\mu \int G d\mu \right|,$$

using the same notations as above. If the system (ϕ_t, μ) is mixing, the rate of approach to zero of $C_t(F,G)$ is called the rate of decay of correlations for its observables F and G. A system exhibits a *slow decay rate of correlations at "short" lags* if the rate is slower than exponential over some characteristic time interval $[0, T]$. This emphasis on the nonuniform decay rate of correlations which leads to modulations of the rate of decay is consistent with the heuristic notion described above and connects the mixing properties of the flow and its power spectral density. In that perspective, the Ruelle–Pollicott resonances [97] might play an important role in the mathematical characterization of the notion of LFV.

The relationships between the two approaches require further study, but we wanted to emphasize here the need for a more precise definition of the notion of LFV encountered in geophysical problems. It appears that the mixing properties of flows encountered in dynamical systems theory offer at least one way to do so.

Appendix C. Hypoellipticity and random SRB measures

To be as self-contained as possible, we recall here the concept of hypoellipticity and its use in the theory of stochastic differential equations. Theorem B of Ledrappier–Young [32] is also restated in a form that is closer to the framework adopted in the present article.

C.1. Hypoellipticity and Hörmander's theorem

Consider an SDE

$$\mathrm{d}X_t = A_0(X)\mathrm{d}t + \sum_{k=1}^{k=d} A_k(X) \circ \mathrm{d}W_t^k \tag{12}$$

in the Stratonovich form [41], where A_0, A_k ($k \in \{1, \ldots, d\}$) are n-dimensional C^∞ vector fields of $\mathbb{R}^n$, and where the W_t^k represent d one-dimensional, independent Wiener processes. It is assumed here that the stochastic flow is well defined for all t.

The Lie bracket of two vector fields V and W is given by

$$[V, W] := \mathrm{D}W \cdot V - \mathrm{D}V \cdot W, \tag{13}$$

where $\mathrm{D}V$ and $\mathrm{D}W$ stand for the usual Jacobian of V and of W in some local coordinates; see for instance [94] and references therein. At each point $x \in \mathbb{R}^n$, Eq. (13) has to be read as

$$[V, W]|_x = DW(x) \cdot V(x) - DV(x) \cdot W(x),$$

and therefore $[\cdot, \cdot]$ is a bilinear operation that associates a vector field $[V, W]$ to the vector fields V and W.

We denote by $\mathfrak{L}\{W_1, \ldots, W_p\}$ the smallest vector space $\mathfrak{G}$ closed under Lie brackets (13), such that $\mathfrak{G}$ contains the vectors $W_1, \ldots, W_p$, i.e. the Lie algebra $\mathfrak{G}$ generated by the vector family $W_1, \ldots, W_p$. We are now in a position to recall Hörmander's celebrated "sum-of-squares theorem" [61,95].

Theorem (*Hörmander*). *Let A_0, A_k ($k \in \{1, \ldots, d\}$) be n-dimensional C^∞ vector fields of $\mathbb{R}^n$ such that Hörmander's condition*

$$\forall\, x \in \mathbb{R}^n \quad \mathfrak{L}\{A_0|_x, [A_1, A_0]|_x, \ldots, [A_d, A_0]|_x\} = \mathbb{R}^n, \tag{14}$$

is satisfied. Then the law of the solutions of Eq. (12), i.e. the probability measure such that $X_t \in \mathrm{d}x$ ($t > 0$), has a C^∞ density with respect to the Lebesgue measure on $\mathbb{R}^n$.

It is interesting to note that A_0 alone represents the drift of Eq. (12), and hence it does not cause any diffusion phenomenon that is required for a density of the process X_t to exist in the usual Fokker–Planck setting. Such diffusion is lacking, for instance, in the case of the Liouville equation (6), which is only a first-order differential operator.

To clarify this statement, we recall here some basic facts related to the hypoellipticity concept and to the Fokker–Planck equation. By using the repeated-index rule for summation, we introduce now the second-order differential operator $\mathcal{L}$ that generates the SDE (12),

$$\mathcal{L} := \frac{1}{2} E^{ij} \partial_{ij} + B^i \partial_i, \tag{15}$$

with E the $n \times n$ matrix whose coefficients are given by

$$E^{ij} := \sum_{k=1}^{k=d} A_k^i A_k^j;$$

here

$$B^i := A_0^i + \frac{1}{2} \sum_{k=1}^{k=d} A_k^j \partial_j A_k^i$$

is the ith-component of the Itô–Stratonovich correction term.

We can thus define the concept of a *hypoelliptic differential operator* for $\mathcal{G} := a^{ij}\partial_{ij} + b^i\partial_i + c$, where a^{ij}, b^i and c are smooth functions from $\mathbb{R}^m$ into $\mathbb{R}$. Let $U \subset \mathbb{R}^m$ and f, g lie in $\mathcal{D}'(U)$, the space of distributions on U, and assume that $\mathcal{G}f = g$ in the distributional sense, i.e.

$$\langle f, \mathcal{G}^*\varphi\rangle = \langle g, \varphi\rangle,$$

for all smooth test functions $\varphi \in \mathcal{D}(U)$ with compact support in U. We call the operator $\mathcal{G}$ *hypoelliptic* if, for all open $V \subset U$,

$$g|_V \in C^\infty(V) \Rightarrow f|_V \in C^\infty(V).$$

Hörmander's remarkable theorem gives sufficient conditions to guarantee the hypoellipticity of $\mathcal{G} = -\partial_t + \mathcal{L}^*$ as an operator on $U = (0, \infty) \times \mathbb{R}^n \subset \mathbb{R}^m$ with $m = n+1$ [95,61]. The hypoellipticity property relaxes the usual ellipticity property that ensures the smoothing effect of a second-order differential operator. In fact, if we assume the operator $\mathcal{L}$ to be *uniformly elliptic*, the vectors $A_1, \ldots, A_d$ already span $\mathbb{R}^n$ at all points, so that Hörmander's condition (14) is always satisfied.

Indeed, assuming that $v \in \{A_1, \ldots, A_d\}^\perp$ implies that, for all $k \in \{1, \ldots, d\}$,

$$0 = \langle v, A_k\rangle^2 = |v^i A_k^i|^2 = v^i A_k^i A_k^j v^j = v^T E v,$$

and we deduce trivially – from the fact that $E = \sigma\sigma^T$ is symmetric and positive definite, with $\sigma = (A_1|\ldots|A_d)$ – that $v \equiv 0$. When $\mathcal{L}$ is not uniformly elliptic, the spanning condition takes the form (14) between the drift part generated by A_0 and the diffusion part generated by $A_1, \ldots, A_d$.

We leave as an exercise the verification of Hörmander's condition in the case of our **[SLM]**. It follows that the law of the process generated by this model has a smooth density on $(0, \infty) \times (\mathbb{R}^3 - \{0\})$.

C.2. Existence of random SRB measures and Ledrappier–Young's theorem

We adapt here the appendix of [32] to the point of view adopted in the present article. It is known that the solutions of (12) are Markov processes that can be represented by $\{\Phi(t, \omega) : \mathbb{R}^n \to \mathbb{R}^n, t \geq 0, \omega \in \Omega\}$, where $\Phi(t, \omega) \in \mathrm{Diff}^\infty(\mathbb{R}^n)$ for each t and ω, $\Phi(t, \omega)$ varies continuously with t for fixed ω, and the transition probabilities $P_t(\cdot|x)$ are given by the distributions of $\omega \to \Phi(t, \omega)$ [41]. Since A_0 and the A_k's are time-independent vector fields, the law of this stochastic semi-flow from time s to time $t > s$ depends only on $t - s$. Thus if ν is the distribution of $\{\Phi(1, \omega),\ \omega \in \Omega\}$, the random diffeomorphisms $\Phi(n, \omega)$ are products of n independent diffeomorphisms with law ν, and we are, therefore, in the framework of the composition of independent random diffeomorphisms considered in [32]. Note that the pair $(\Phi(n, \omega), \theta)$ – with θ being the shift operator at time 1 acting on the Wiener space described in Section 3.1 – form a discrete RDS associated with the SDE (12); see [29].

Theorem B of [32] can now be reformulated as follows, in the light of Appendix C.1.

Theorem (*Corollary of Ledrappier and Young [32]*). *Consider an SDE (12) with smooth vector fields A_0 and A_k, $k \in \{1, \ldots, d\}$, such that the discrete RDS $(\Phi(n, \omega), \theta)$ above possesses a random global attractor. Assume that the Hörmander condition (14) is satisfied and that there exists a positive Lyapunov exponent associated with (12). Then the sample measures associated with the discrete RDS $(\Phi(n, \omega), \theta)$, have the SRB property.*

To prove this theorem it suffices to note that the $P_1(\cdot|x)$'s have C^∞ densities with respect to Lebesgue measure, by Hörmander's theorem, and to use Theorem B of [32]. The theorem thus obtained applies to our **[SLM]**.

Please cite this article in press as: M.D. Chekroun, et al., Stochastic climate dynamics: Random attractors and time-dependent invariant measures, Physica D (2011), doi:10.1016/j.physd.2011.06.005

Appendix D. Supplementary data

Supplementary material related to this article can be found online at doi:10.1016/j.physd.2011.06.005.

References

[1] V.I. Arnol'd, Geometrical Methods in the Theory of Ordinary Differential Equations, Springer-Verlag, New York, 1983.
[2] J.-P. Eckmann, D. Ruelle, Ergodic theory of chaos and strange attractors, Rev. Modern Phys. 57 (1985) 617–656.
[3] E.N. Lorenz, Deterministic nonperiodic flow, J. Atmos. Sci. 20 (1963) 130–141.
[4] K. Hasselmann, Stochastic climate models, part 1: theory, Tellus 28 (1976) 473–485.
[5] M. Ghil, Hilbert problems for the geosciences in the 21st century, Nonlinear Process. Geophys. 8 (2001) 211–222.
[6] E. Kalnay, Atmospheric Modeling, Data Assimilation and Predictability, Cambridge University Press, 2003.
[7] S. Solomon, et al., Climate Change 2007: The Physical Science Basis. Contribution of Working Group I to the Fourth Assessment Report of the IPCC, Cambridge University Press, 2007.
[8] A.J. Chorin, O.H. Hald, R. Kupferman, Optimal prediction with memory, Physica D 166 (2002) 239–257.
[9] R. Kleeman, A. Majda, I. Timofeyev, Quantifying predictability in a model with statistical features of the atmosphere, Proc. Natl. Acad. Sci. USA 99 (2002) 15291–15296.
[10] C. Penland, P.D. Sardeshmukh, The optimal growth of tropical sea-surface temperature anomalies, J. Clim. 8 (1995) 1999–2024.
[11] C. Penland, Stochastic linear models of nonlinear geosystems, in: A.A. Tsonis, J.B. Elsner (Eds.), Nonlinear Dynamics in Geosciences, Springer-Verlag, 2007.
[12] S. Kravtsov, D. Kondrashov, M. Ghil, in: T.N. Palmer, P. Williams (Eds.), Stochastic Physics and Climate Modelling, Cambridge University Press, 2009, pp. 35–72.
[13] D. Ruelle, F. Takens, On the nature of turbulence, Commun. Math. Phys. 20 (1971) 167–192.
[14] L.-S. Young, What are SRB measures, and which dynamical systems have them? J. Stat. Phys. 108 (2002) 733–754.
[15] M. Ghil, A.W. Robertson, Solving problems with GCMs: general circulation models and their role in the climate modeling hierarchy, in: D. Randall (Ed.), General Circulation Model Development: Past, Present and Future, Academic Press, San Diego, 2000, pp. 285–325.
[16] I.M. Held, The gap between simulation and understanding in climate modeling, Bull. Am. Meteorol. Soc. 86 (2005) 1609–1614.
[17] J.C. McWilliams, Irreducible imprecision in atmospheric and oceanic simulations, Proc. Natl. Acad. Sci. USA 104 (2007) 8709–8713.
[18] G.L. Eyink, T.W.N. Haine, D.J. Lea, Ruelle's linear response formula, ensemble adjoints schemes, and Lévy flights, Nonlinearity 17 (2004) 1867–1889.
[19] A.S. Gritsoun, Fluctuation-dissipation theorem on attractors of atmospheric models, Russian J. Numer. Anal. Math. Modelling 16 (2001) 97–190.
[20] A.S. Gritsoun, G. Branstator, V.P. Dymnikov, Construction of the linear response operator of an atmospheric general circulation model to small external forcing, Russian J. Numer. Anal. Math. Modelling 17 (2002) 399–416.
[21] A.S. Gritsoun, G. Branstator, Climate response using a three-dimensional operator based on the fluctuation dissipation theorem, J. Atmospheric Sci. 64 (2007) 2558–2575.
[22] R. Abramov, A. Majda, A new algorithm for low frequency climate response, J. Atmospheric Sci. 66 (2009) 286–309.
[23] R. Buizza, M. Miller, T.N. Palmer, Stochastic representation of model uncertainties in the ECMWF ensemble prediction system, Q. J. Roy. Meteorol. Soc. 125 (1999) 2887–2908.
[24] J.D. Neelin, O. Peters, J.W.-B. Lin, K. Hales, C.E. Holloway, CE rethinking convective quasi-equilibrium: observational constraints for stochastic convective schemes in climate models, Phil. Trans. Roy. Soc. London A 366 (2008) 2581–2604.
[25] M. Ghil, Cryothermodynamics: the chaotic dynamics of paleoclimate, Physica D 77 (1994) 130–159.
[26] B. Saltzman, Dynamical Paleoclimatology, Academic Press, 2002.
[27] F.-F. Jin, J.D. Neelin, M. Ghil, El Niño on the devil's staircase: annual subharmonic steps to chaos, Science 264 (1994) 70–72.
[28] E. Tziperman, L. Stone, M. Cane, J. Jarosh, El Niño chaos: overlapping of resonances between the seasonal cycle and the Pacific ocean–atmosphere oscillator, Science 264 (1994) 72–74.
[29] L. Arnold, Random Dynamical Systems, Springer-Verlag, NY, 1998.
[30] D. Cheban, Global attractors of nonautonomous dissipative dynamical systems, in: Interdisciplinary Mathematical Sciences, World Scientific, 2004.
[31] M. Ghil, M.D. Chekroun, E. Simonnet, Climate dynamics and fluid mechanics: natural variability and related uncertainties, Physica D 237 (2008) 2111–2126.
[32] F. Ledrappier, L.-S. Young, Entropy formula for random transformations, Probab. Theory Related Fields 80 (1988) 217–240.
[33] F.-F. Jin, An equatorial ocean recharge paradigm for ENSO. Part II: a stripped-down coupled model, J. Atmospheric Sci. 54 (1997) 830–847.
[34] H. Crauel, Random Probability Measures on Polish Spaces, in: The Stochastic Monographs: Theory and Applications of Stochastic Process Series, vol. 11, Taylor & Francis, 2002.
[35] V.S. Anishchenko, T.E. Vadivasova, A.S. Kopeikin, G.I. Strelkova, J. Kurths, Influence of noise on statistical properties of nonhyperbolic attractors, Phys. Rev. E 62 (2000) 7886–7893.
[36] H.A. Dijkstra, Nonlinear Physical Oceanography: A Dynamical Systems Approach to the Large Scale Ocean Circulation and El Niño, 2nd ed., Springer-Verlag, NY, 2005.
[37] L. Sushama, M. Ghil, K. Ide, Spatio-temporal variability in a mid-latitude ocean basin subject to periodic wind forcing, Atmos.-Ocean 45 (2007) 227–250.
[38] J.D. Neelin, et al., ENSO theory, J. Geophys. Res. 103 (1998) 14261–14290.
[39] A.V. Fedorov, S.L. Harper, S.G. Philander, B. Winter, A. Wittenberg, How predictable is El Niño? Bull. Am. Meteorol. Soc. 84 (2003) 911–919.
[40] A. Timmermann, F.-F. Jin, A nonlinear mechanism for decadal El Niño amplitude changes, Geophys. Res. Lett. 29 (2002) 1003. doi:10.10129/2001GL13369.
[41] H. Kunita, Stochastic Flows and Stochastic Differential Equations, Cambridge Univ. Press, 1990.
[42] H. Crauel, G. Dimitroff, M. Scheutzow, Criteria for strong and weak random attractors, J. Dynam. Differential Equations 21 (2009) 233–247.
[43] H. Crauel, Random point attractors versus random set attractors, J. Lond. Math. Soc. 63 (2001) 413–427.
[44] H. Crauel, F. Flandoli, Attractors for random dynamical systems, Probab. Theory Related Fields 100 (1994) 365–393.
[45] H. Crauel, White noise eliminates instablity, Arch. Math. 75 (2000) 472–480.
[46] H. Crauel, F. Flandoli, Additive noise destroys a pitchfork bifurcation, J. Dynam. Differential Equations 10 (1998) 259–274.
[47] P. Ashwin, Attractors of a randomly forced electronic oscillator, Physica D 125 (1999) 302–310.
[48] M. Ghil, S. Childress, Topics in Geophysical Fluid Dynamics: Atmospheric Dynamics, Dynamo Theory and Climate Dynamics, Springer, 1987.
[49] S.E. Zebiak, M.A. Cane, A model El Niño–Southern Oscillation, Mon. Weather Rev. 115 (1987) 2262–2278.
[50] N. Ohtomo, et al., Exponential characteristics of power spectral densities caused by chaotic phenomena, J. Phys. Soc. Japan 64 (1995) 1104–1113.
[51] A. Timmermann, F.-F. Jin, J. Abshagen, A nonlinear theory for El Niño bursting, J. Atmospheric Sci. 60 (2003) 152–165.
[52] M. Ghil, et al., Advanced spectral methods for climatic time series, Rev. Geophys. 40 (1) (2002) pp. 3.1–3.41.
[53] K. Bhattacharya, M. Ghil, I.L. Vulis, Internal variability of an energy-balance model with delayed albedo effects, J. Atmospheric Sci. 39 (1982) 1747–1773. doi:10.1175/1520-0469.
[54] J. Guckenheimer, P. Holmes, Nonlinear Oscillations, Dynamical Systems, and Bifurcations of Vector Fields, Springer-Verlag, NY, 1983.
[55] Y. Kifer, Ergodic Theory of Random Perturbations, Birkhäuser, 1988.
[56] P. Collet, C. Tresser, Ergodic theory and continuity of the Bowen-Ruelle measure for geometrical flows, Fyzika 20 (1988) 33–48.
[57] W. Tucker, Lorenz attractor exists, C.R. Acad. Sci. Paris 328 (12) (1999) 1197–1202.
[58] V. Araujo, M. Pacifico, R. Pujal, M. Viana, Singular-hyperbolic attractors are chaotic, Trans. Amer. Math. Soc. 361 (2009) 2431–2485.
[59] M. Dorfle, R. Graham, Probability density of the Lorenz model, Phys. Rev. A 27 (1983) 1096–1105.
[60] A.K. Mittal, S. Dwivedi, R.S. Yadav, Probability distribution for the number of cycles between successive regime transitions for the Lorenz model, Physica D 233 (2007) 14–20.
[61] Denis R. Bell, Degenerate Stochastic Differential Equations and Hypoellipticity, Longman, Harlow, 1995.
[62] A. Lasota, M.C. Mackey, Chaos, Fractals, and Noise: Stochastic Aspects of Dynamics, in: Applied Mathematical Sciences, vol. 97, Springer-Verlag, New York, 1994.
[63] J.J. Kohn, Pseudo-differential operators and hypoellipticity, Proc. Amer. Math. Soc. Symp. Pure Math. 23 (1973) 61–69.
[64] C. Soize, The Fokker–Planck Equation for Stochastic Dynamical Systems and its Explicit Steady State Solutions, World Scientic Publishing Co., 1994.
[65] A.N. Carvalho, J.A. Langa, J.C. Robinson, Lower semicontinuity of attractors for non-autonomous dynamical systems, Ergodic Theory Dynam. Systems 29 (2009) 1765–1780.
[66] R. Rajaram, Exact boundary controllability of the linear advection equation, Appl. Anal. 88 (1) (2009) 121–129.
[67] M. Dellnitz, O. Junge, On the approximation of complicated dynamical behavior, SIAM J. Numer. Anal. 36 (2) (1999) 491–515.
[68] G. Froyland, Finite approximation of Sinai–Bowen–Ruelle measures for Anosov systems in two dimensions, Random Comput. Dyn. 3 (1995) 251–263.
[69] J. Ding, A. Zhou, Finite approximation of Frobenius–Perron operators, a solution of Ulam's conjecture to multi-dimensional transformation, Physica D 92 (1–2) (1996) 61–66.
[70] M. Dellnitz, G. Froyland, C. Horenkamp, K. Padberg-Gehle, A.S. Gupta, Seasonal variability of the subpolar gyres in the Southern Ocean: a numerical investigation based on transfer operators, Nonlinear Process. Geophys. 16 (2009) 655–664.
[71] S. Ulam, Problems in Modern Mathematics, Interscience, New York, 1960.
[72] G. Osipenko, Symbolic images and invariant measures of dynamical systems, Ergodic Theory Dynam. Systems 30 (2010) 1217–1237. doi:10.1017/S0143385709000431.
[73] D. Julitz, Numerical approximation of atmospheric-ocean models with subdivision algorithm, Discrete Contin. Dyn. Syst. 18 (2007) 429–447.

[74] G. Froyland, S. Lloyd, N. Santitissadeekorn, Coherent sets for nonautonomous dynamical systems, Physica D 239 (2010) 1527–1541.
[75] M. Dellnitz, A. Hohmann, O. Junge, M. Rumpf, Exploring invariant sets and invariant measures, Chaos 7 (1997) 221–228.
[76] M. Dellnitz, A. Hohmann, A subdivision algorithm for the computation of unstable manifolds and global attractors, Numer. Math. 75 (1997) 293–317.
[77] B.P. Kirtman, P.S. Schopf, Decadal variability in ENSO predictability and prediction, J. Clim. 11 (1998) 2804–2822.
[78] D.Z. Sun, in: H.F. Diaz, V. Markgraf (Eds.), El Niño: Historical and Paleoclimatic Aspects of the Southern Oscillation, Multiscale Variability and Global and Regional Impacts, Cambridge University Press, 2000, pp. 443–463.
[79] M. Ghil, N. Jiang, Recent forecast skill for the El Niño/southern oscillation, Geophys. Res. Lett. 25 (1998) 171–174.
[80] J. Guckenheimer, C. Kuehn, Homoclinic orbits of the FitzHugh-Nagumo equation: bifurcations in the full system, SIAM J. Appl. Dyn. Syst. 8 (3) (2009) 138–153.
[81] H. Zhao, Z.-H. Zheng, Random periodic solutions of random dynamical systems, J. Differential Equations 246 (2009) 2020–2038.
[82] C. Penland, A stochastic model of IndoPacific sea surface temperatures using linear inverse modeling, Physica D 98 (1996) 534–558.
[83] V. Baladi, Spectrum and statistical properties of chaotic dynamics, Progr. Math. 201 (2001) 203–223.
[84] M. Ghil, A.W. Robertson, "Waves" vs. "particles" in the atmosphere's phase space: a pathway to long-range forecasting? Proc. Natl. Acad. Sci. USA 99 (2002) 2493–2500.
[85] D. Ruelle, A review of linear response theory for general differentiable dynamical systems, Nonlinearity 22 (2009) 855–870.
[86] C. Leith, Climate response and fluctuation dissipation, J. Atmospheric Sci. 32 (1975) 2022–2026.
[87] V. Lucarini, Response theory for equilibrium and non-equilibrium statistical mechanics: causality and generalized Kramers-Kronig relations, J. Stat. Phys. 131 (2008) 543–558.
[88] D. Ruelle, Differentiation of SRB states for hyperbolic flows, Ergodic Theory Dynam. Systems 28 (2008) 613–631.
[89] A. Majda, M. Hairer, A simple framework to justify linear response theory, Nonlinearity 23 (4) (2010) 909–922.
[90] Y. Kifer, V.M. Gundlach, Random hyperbolic systems, in: H. Crauel, M. Gundlach (Eds.), Stochastic Dynamics, Springer-Verlag, 1999, pp. 117–145.
[91] J. Duan, B. Schmalfuss, The 3D quasigeostropic fluid dynamics under random forcing on boundary, Commun. Math. Sci. 1 (1) (2003) 133–151.
[92] B. Blanke, J.D. Neelin, D. Gutzler, Estimating the effect of stochastic wind stress forcing on ENSO irregularity, J. Climate 10 (1997) 1473–1486.
[93] T. Bogenschütz, Z.S. Kowalski, A condition for mixing of skew products, Aequationes Math. 59 (2000) 222–234.
[94] M.D. Chekroun, M. Ghil, J. Roux, F. Varadi, Averaging of time-periodic systems without a small parameter, Discrete Contin. Dyn. Syst. A 14 (4) (2006) 753–782.
[95] L. Hörmander, Hypoelliptic second order differential equations, Acta Math. 119 (1967) 147–171.
[96] M.D. Chekroun, D. Kondrashov, M. Ghil, Predicting stochastic systems by noise sampling, and application to the El Nino-Southern Oscillation, Proc. Natl. Acad. Sci. USA 108 (29) (2011) 11766–11771. doi:10.1073/pnas.1015753108.
[97] D. Ruelle, Resonances of chaotic dynamical systems, Phys. Rev. Lett. 56 (5) (1986) 405–407.

Please cite this article in press as: M.D. Chekroun, et al., Stochastic climate dynamics: Random attractors and time-dependent invariant measures, Physica D (2011), doi:10.1016/j.physd.2011.06.005